AD-A282 494

CLEARED
FOR OPEN PUBLICATION
except for page 3
which was not provided.
JUL 18 1994 12

DIRECTORATE FOR FREEDOM OF INFORMATION
AND SECURITY REVIEW (OASD-PA)
DEPARTMENT OF DEFENSE

FINAL TECHNICAL REPORT
DIODE-PUMPED
MICRO-LASER ARRAYS

DTIC
ELECTE
JUL 25 1994
S
F

Sponsored by

Advanced Research Projects Agency

Defense Sciences Office

Diode-Pumped Micro-Laser Arrays

ARPA Order No. 8778

Issued by ARPA/CMO under Contract #MDA972-92-C-0047

This document has been approved for public release and sale; its distribution is unlimited

"The views and conclusions contained in this document are those of the authors and should not be interpreted as representing the official policies, either expressed or implied, of the Defense Advanced Research Projects Agency or the U.S. Government."

DTIC QUALITY INSPECTED 5

94-23209

9

94 7 22 188

94-S-2581

REPORT DOCUMENTATION PAGE

Form Approved
OMB No. 0704-0188

Public reporting burden for this collection of information is estimated to average 1 hour per response, including the time for reviewing instructions, searching existing data sources, gathering and maintaining the data needed, and completing and reviewing the collection of information. Send comments regarding this burden estimate or any other aspect of this collection of information, including suggestions for reducing this burden, to Washington Headquarters Services, Directorate for Information Operations and Reports, 1215 Jefferson Davis Highway, Suite 1204, Arlington, VA 22202-4302, and to the Office of Management and Budget, Paperwork Reduction Project (0704-0188), Washington, DC 20503.

1. AGENCY USE ONLY (Leave blank)	2. REPORT DATE	3. REPORT TYPE AND DATES COVERED
	6-1-94	FINAL, 9/30/93 - 2/18/94

4. TITLE AND SUBTITLE
DIODE-PUMPED MICRO-LASER ARRAYS

5. FUNDING NUMBERS
MDA-972-92-C-0047

6. AUTHOR(S)
R WAARTS

7. PERFORMING ORGANIZATION NAME(S) AND ADDRESS(ES)
SDL, INC.
80 ROSE ORCHARD WAY
SAN JOSE, CA 95134-1365

8. PERFORMING ORGANIZATION REPORT NUMBER

9. SPONSORING/MONITORING AGENCY NAME(S) AND ADDRESS(ES)
ARPA
3701 N. FAIRFAX DRIVE
ARLINGTON, VA 22203-1714

10. SPONSORING/MONITORING AGENCY REPORT NUMBER

11. SUPPLEMENTARY NOTES
PREPARED UNDER CONTRACT MDA-972-92-C-0047

12a. DISTRIBUTION/AVAILABILITY STATEMENT

b. DISTRIBUTION CODE

13. ABSTRACT *(Maximum 200 words)*
SEE ATTACHED

14. SUBJECT TERMS
LASER DIODES, 2-D ARRAYS, SOLID STATE LASERS, MICRO-LASERS

15. NUMBER OF PAGES
39

16. PRICE CODE

17. SECURITY CLASSIFICATION OF REPORT	18. SECURITY CLASSIFICATION OF THIS PAGE	19. SECURITY CLASSIFICATION OF ABSTRACT	20. LIMITATION OF ABSTRACT
UNCL	UNCL	UNCL	

NSN 7540-01-280-5500

Standard Form 298 (Rev. 2-89)
Prescribed by ANSI Std. Z39-18
298-102

Abstract

In this work SDL investigated the operation of 2-D high power micro-laser arrays based on novel monolithic surface-emitting laser diode arrays coupled to Yb:YAG and Er:YSGG micro-laser crystals.

The experimental demonstrations include 1) 200 mW, q-cw single Yb:YAG microlaser, 2) 930 mW cw linear, 12-element Er:YSGG micro-laser, 3) 130 Watt q-cw 2-D surface-emitting laser diode array at 970 nm, and 4) 600 mW, q-cw from an 18-element 2-D Er:YSGG microlaser array.

The experiments performed at SDL under this contract demonstrate the suitability of monolithic 2-D laser diode arrays for pumping solids state lasers. In addition, the experiments show the flexibility of the micro-laser concept. Using different pump wavelengths in combination with different micro-lasers a wide output wavelength range from 1 micron to 3 micron is demonstrated. Finally, the micro-laser array is shown to be scalable by exploiting one- and two-dimensional laser diode pump arrays.

Accesion For
NTIS CRA&I ☑
DTIC TAB ☐
Unannounced ☐
Justification .....
By .....
Distribution /
Availability Codes
Dist | Avail and / or Special
A-1

Final Report on

DIODE-PUMPED MICRO-LASER ARRAYS

Contract # MDA-972-92-C-0047

May 1994

Prepared by:

Robert G. Waarts,

Staff Scientist, SDL Inc.,

80 Rose Orchard Way, San Jose, CA 95134

Tel: (408) 943-9411 FAX: (408) 943-1070

TABLE OF CONTENTS

SUMMARY

In this work SDL investigated the operation of 2-D high power micro-laser arrays based on novel monolithic surface emitting laser diode arrays coupled to Yb:YAG and Er:YSGG micro-laser crystals . The following results were demonstrated:

1) Yb:YAG micro-lasers were demonstrated pumped with single edge-emitting laser diodes operating at a wavelength of 940 nm. Butt-coupling of the laser diode to the Yb:YAG micro-laser resulted in 200 mW q-cw output power from the micro-laser at 1.03 micron. No cw operation was demonstrated, due to thermal effects in Yb:YAG.

2) A linear Er:YSGG micro-laser array was demonstrated with 930 mW cw total output power at 2.8 micron. The linear micro-laser array was pumped with a 1 cm wide edge emitting laser diode array with a maximum total output power of 15 watt.

3) Two-dimensional (4x12 element) monolithic, surface-emitting laser diode arrays were demonstrated. 132 W q-cw total output power was obtained at 973 nm wavelength from an array of surface emitting lasers with dry etched 90° and 45° facets. This is the highest power level ever demonstrated from a surface-emitting laser array. Furthermore, 3.4 W cw output power has been achieved from a single surface emitting laser.

4) A 48 element 2-D micro-laser array with 600 mW q-cw output power at 2.8 micron pumped by a monolithic 2-D laser diode array was demonstrated. The output efficiency of the micro-laser could be further improved with the use of beam shaping micro-optics between the laser diode array and the micro-laser as was demonstrated in separate experiments based on a linear array of laser diodes.

The experiments performed at SDL under this contract demonstrate the suitability of monolithic 2-D laser diode arrays for pumping solids state lasers. In addition, the experiments show the flexibility of the micro-laser concept. Using different pump wavelengths in combination with different micro-lasers a wide output wavelength range from 1 micron to 3 micron is demonstrated. Finally, the micro-laser array is shown to be scalable by exploiting one- and two-dimensional laser diode pump arrays.

I. INTRODUCTION

Diode-pumped solid state micro-lasers with short monolithic resonators permit the fabrication of compact and simple solid state lasers.[1] These compact solid state lasers are comprised of a thin solid state gain medium polished flat on both sides and reflectors coated or otherwise attached to the input and output facet of the gain medium. Several different micro-lasers have been demonstrated using Nd:YAG as well as other solid state materials and are becoming commercially available. In addition to the advantages associated with single micro-lasers one of the advantages of the micro-laser concept, is that it can easily be extended to arrays of micro-lasers. One dimensional arrays of micro-lasers have been demonstrated with a linear laser diode bar [2,3] and high power 2-D operation has been demonstrated based on a 5 stack laser diode bars.[4] Although the output power from the these micro-laser arrays is not diffraction limited, the brightness remains very high and may be suitable for applications such as, for example, material processing and medical application. The configuration of the 2-D micro-laser array is uniquely suited for the combination with recently developed monolithic 2-D arrays of surface emitting laser diodes.[5,10]

The goal of this program is to investigate 2-D micro-laser arrays based on monolithic 2-D surface emitting laser diode arrays optically coupled to a micro-laser cavity. The design of the micro-laser array is presented in Figure 1. The laser array consists of basically two components, the 2-D laser diode array and the micro-laser cavity. The 2-D laser diode array is comprised of a monolithic array of surface emitting lasers. The semiconductor laser cavity is defined by a 90° ion milled facet with a high reflection coating and a distributed Bragg reflector or alternatively superlattice reflector integrated with the epitaxial structure and positioned just above the 45° mirror. The light from the 45° mirror is coupled through the surface out of the anti reflection coated surface of the laser diode array. The laser diode array is bonded p-side down on a water cooled heat sink for high power operation. To avoid absorption in the substrate the emission wavelength of the laser arrays is greater than 920 nm. Shorter wavelength operation of the laser array may be achieved by etching off the substrate above the area of laser emission.

The light from the laser diode array is coupled to a solid state micro-laser array. Two different micro-laser arrays were investigated in this program, Yb:YAG lasing at 1.03 micron and Er:YSGG lasing at 2.8 micron. The micro-laser cavity has two parallel flat surfaces which are the reflectors of the laser cavity. Our initial experiments used a Yb doped YAG micro-laser. The Yb doped YAG laser is pumped at around 940 nm wavelength and oscillates at 1.03 micron. The relatively long pump wavelength of 940 nm is suitable for transmission of the pump light through the GaAs substrate. In addition, the long pump wavelength results in a relatively low quantum defect for potentially high pump efficiency. A disadvantage of the Yb:YAG micro-laser is that it is a quasi three level system, which results in a relatively high threshold pump power. Our experimental results demonstrate the operation of single laser diode-pumped Yb:YAG micro-lasers with output power over 200 mW under pulsed operation with a diffraction limited output beam. However, we found that

THIS PAGE IS MISSING IN ORIGINAL DOCUMENT

Page 3
Figure 1

II. EXPERIMENTAL RESULTS Yb:YAG MICRO CAVITY

In this section, we will discuss the experimental results obtained from diode-pumped Yb:YAG lasers. Figure 2 shows the measured absorption and fluorescence of Yb:YAG as a function of wavelength. The insert shows a partial energy diagram. The absorption spectrum shows two large absorption peaks; a relatively broad absorption peak with a 10 nm width is centered at around 940 nm and a second narrower peak, which is several nm wide, is centered around 970 nm. The main advantages of Yb:YAG are:

a) The high quantum efficiency based on a 940 nm pump wavelength results in a theoretical optical to optical efficiency of 90%.

b) The absorption spectrum at around 940 nm is much broader as compared to other solid state laser systems. Therefore the light from a laser diode is more efficiently absorbed as the laser changes wavelength, for example, with temperature changes of the laser, or in the case of arrays when the spectrum from the laser diode array varies from one element to the other.

c) The dopant concentration of Yb:YAG can be much higher as compared to other solid state laser systems, such as Nd:YAG. Dopant concentration of 25 to 50 % have been demonstrated as opposed to only several percent dopant concentration for other solid state lasers. The high dopant concentration leads to a shorter absorption length for the pump beam. The short absorption length has several advantages. Firstly, without the use of micro-optics between the laser diode and the micro-laser the light from the laser diode is rapidly diverging. By reducing the length of the micro-laser, the laser diode light may be sufficiently confined over the short interaction length to be able to operate without micro-optics between the laser diode array and the micro-laser. A second advantage of the light Yb dopant concentration is that the short cavity results in a reduction of the linear losses in the cavity.

d) The 940 nm pump wavelength is compatible with the surface emitting laser arrays which require wavelengths longer than 920 nm for efficient transmission through the GaAs substrate.

Although the Yb:YAG has many advantages, it also has a serious disadvantage. The Yb:YAG is a quasi three level system because the lower lasing state is within the ground state manifold. Depending on temperature, the lower lasing level has a significant population due to the thermal distribution of the ground level. To obtain inversion between the upper and lower lasing levels and obtain gain, it is therefore necessary to pump this three level system much harder as compared to a four level system such as Nd:YAG.

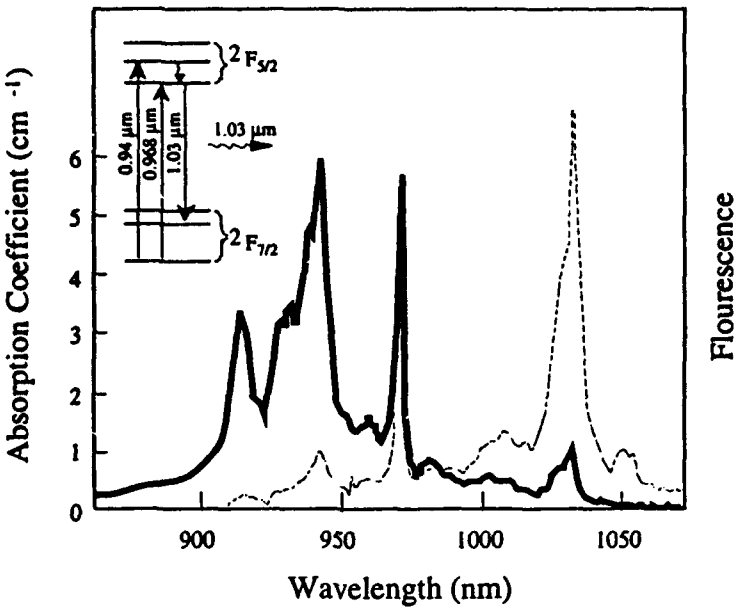

Figure 2: Absorption coefficient and fluorescence of Yb:YAG as a function of wavelength.

II.1. Yb:YAG MICRO-LASER PUMPED WITH A TI:SAPPHIRE LASER

Yb:YAG crystals were procured from Scientific Materials Corp. The crystals were cut and polished to a size of 3 by 6 mm. The thickness of the crystal is different for the two different dopant concentrations of the Yb. For a 25 % doped crystal the thickness is 250 micron and for a 25 % doped crystal the thickness was chosen to be 450 micron. The thickness of the two different crystals results in 90 % absorption in the crystal, The surface flatness is less than 1/10 th wavelength and the wedge is less than 3 arc min.

The Yb:YAG crystals were coated by Thin Film Labs. A schematic diagram of the coated crystals together with the coating specifications is given in Figure 3. The coating was specified with a 95 % reflective output mirror at both the pump and lasing wavelength and a back mirror with high transmission (>90 %) at the pump wavelength and high reflection (>99 %) at the lasing wavelength. While the 95 % reflective output mirror coating is easy to fabricate, the coating for the mirror through which the pump beam is coupled into the cavity is more difficult. The measured reflectivity of the coating on a test sample positioned close to the actual sample is shown in Figure 4. As can be seen from this Figure, small changes in wavelength around the 940 nm pumping wavelength may result in large changes in reflectivity. Similarly, small change in the process parameters during the fabrication of the coating may result in large changes in the reflectivity of the coating at the pump wavelength.

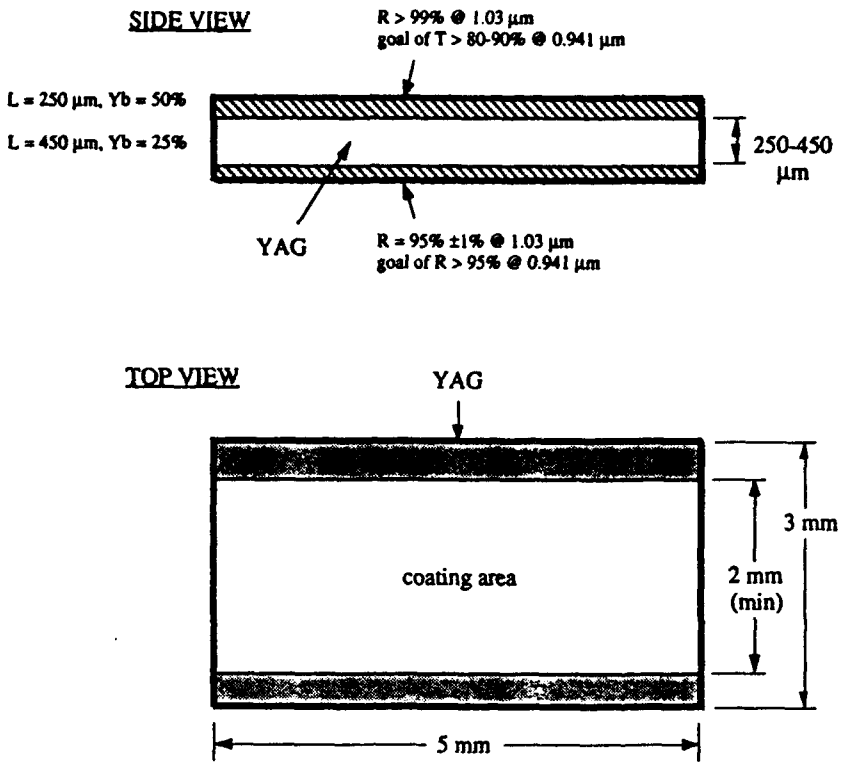

Figure 3 : Coating specifications for Yb:YAG micro-laser.

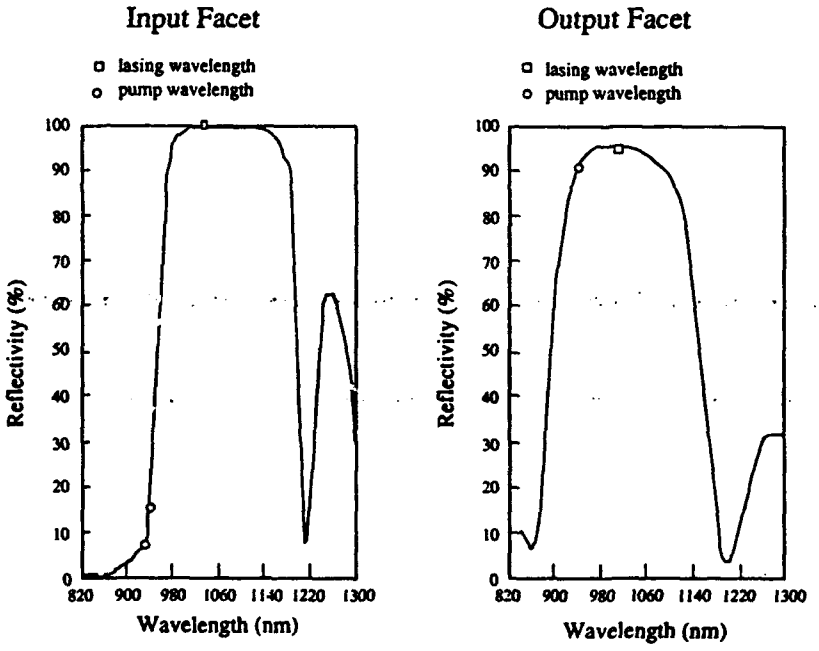

Figure 4: Measured reflectivity of the coatings of the Yb:YAG micro-laser.

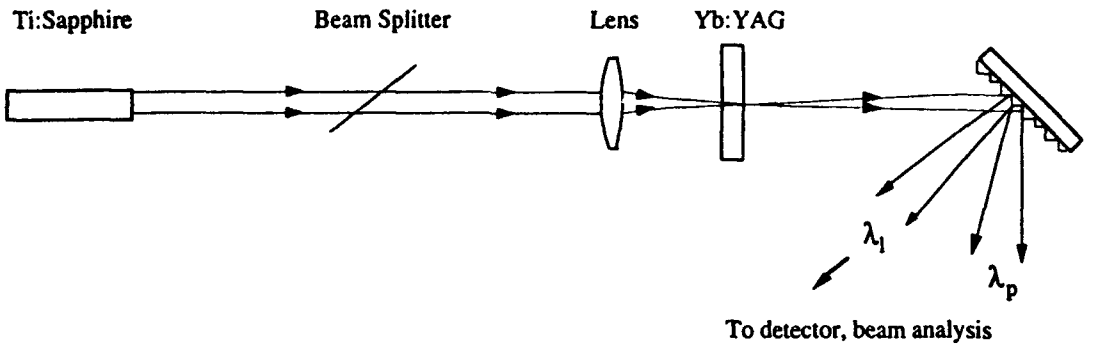

Figure 5: Schematic diagram of the experimental set-up for testing Yb:YAG micro-lasers with a Ti:Sapphire laser.

To test the Yb:YAG micro cavity we focused the output from a Ti:Sapphire laser on to the Yb:YAG crystal. Both the 25 % Yb and 50 % doped Yb cavities were tested. A schematic diagram of the experimental set up is shown in Figure 5. The light from the 450 mW maximum output power Ti:Sapphire laser was focused on the Yb:YAG micro cavity with a single focusing lens. By changing the focal length of the lens, we optimized the size of the focused spot at the micro cavity. The best results were obtained with a 25 μm spot. At this spot size, the beam remains focused over a length of 1 mm which exceeds the length of both the 25 % and 50 % Yb-doped cavities. The power at the 1030 nm output wavelength was monitored as a function of the pump wavelength. No lasing was observed for the 50 % doped Yb:YAG cavity. The reason is most likely the quenching of the gain in the material at this doping concentration. This has also later been observed independently by other researchers at MIT-LL.

The output power at the 1030 nm lasing wavelength as a function of the pump power for the 25 % doped Yb:YAG cavity, for two different pump wavelengths, is shown in Figure 6. For a pump wavelength of 930 nm the lasing threshold is 200 mW and a maximum output power of 110 mW is obtained at a pump power of 450 mW. At the 940 nm pump wavelength the pump threshold power is 350 mW. At pumping wavelengths longer than 940 nm, no lasing was observed. These results are in contradiction with our expectations based on the known absorption bandwidth of Yb:YAG. The measured absorption spectrum of Yb:YAG has a peak at 940 nm with a bandwidth of approximately 20 nm. Therefore, we would have expected to absorb the pump beam most efficiently at a wavelength of 940 nm and as a result obtain the best lasing threshold and output power at this pump wavelength. We speculate that the reason for the observed lower efficiency at the 940 nm pump wavelength is the higher reflectivity of the coating as shown in Figure 4. Very small changes in the coating process may have shifted the coating over to a shorter wavelength, resulting in a large reflection at the pump wavelength.

We measured the spectrum from the Yb:YAG cavity at a pump wavelength of 930 nm. Figure 6b shows the measured spectra at a pump power of 250 and 440 mW. The measured spectrum has multi-longitudinal modes which are spaced at 0.62 micron. The spacing

between the modes corresponds well with the spacing of the cavity modes determined by the 450 micron long cavity with an index of 1.8. Finally, we measured the far field from the laser, shown in Figure 6c. The far field is near-Gaussian and symmetric.

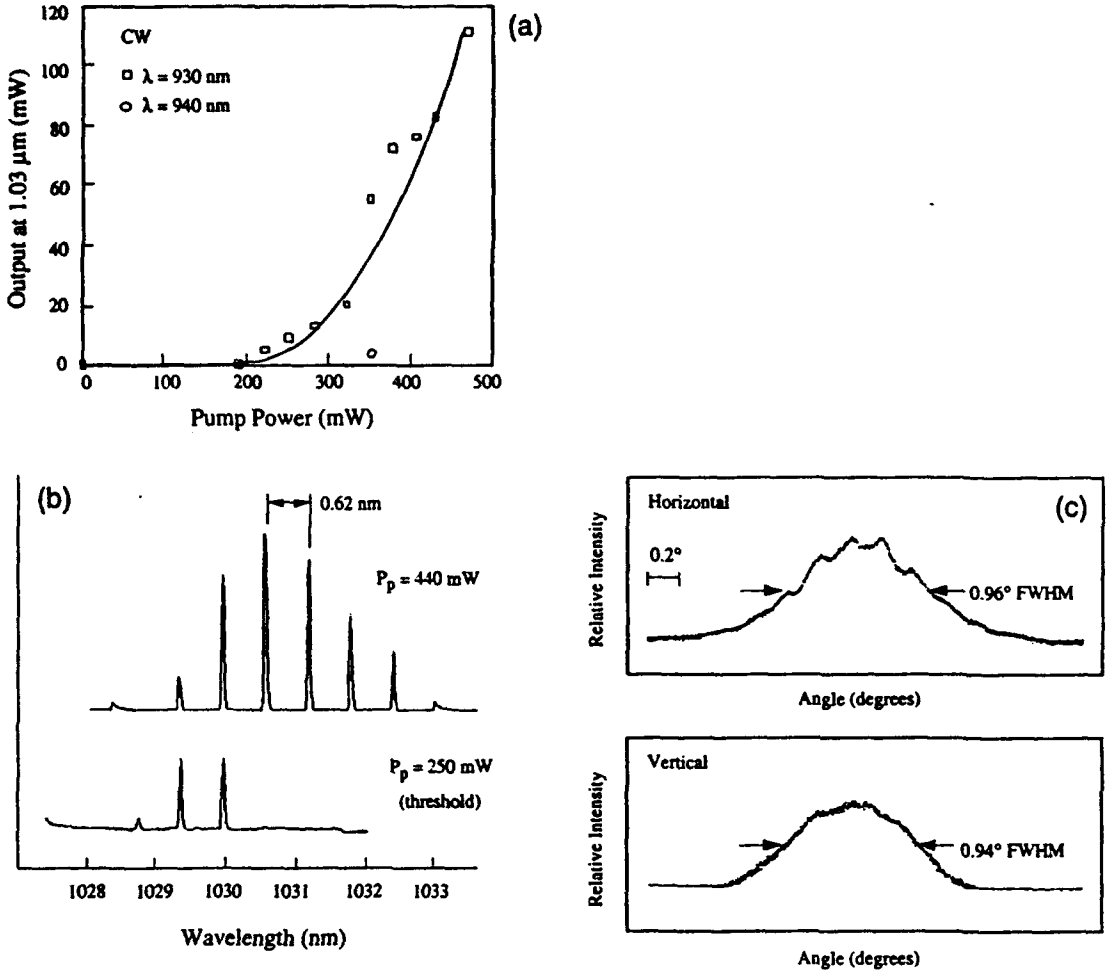

Figure 6: Summary of experimental results for a Yb:YAG micro-laser pumped with a Ti:Sapphire laser.

In a second series of experiments, 5 by 5 mm Yb:YAG crystals were fabricated. The 25 % doped crystals were polished to a thickness of 450 micron. The crystals were coated with special attention given to the coating of the pump mirror. The Yb:YAG cavity was tested with the Ti:Sapphire laser as in the previously described experiments. Figure 7 summarizes the experimental results. A maximum output power of 40 mW was obtained at a maximum input power from the Ti:Sapphire laser of 350 mW and a pump wavelength of 940 nm. The maximum output power was limited by the output power from the Ti:Sapphire laser at this wavelength. These measured results are in good agreement with the measured absorption spectrum of Yb:YAG with a peak absorption around 940 nm.

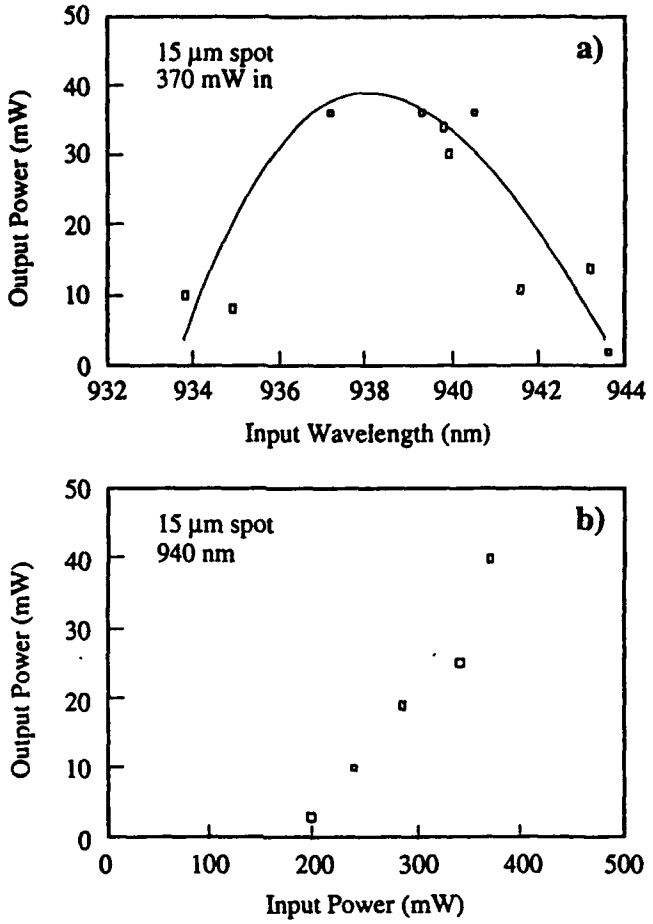

Figure 7: Summary of results for the Yb:YAG micro-laser with improved coating: a) output power as a function of wavelength, b) output power as a function of pump power.

Scanning the pump wavelength and observing the output power we also observed that the output power at 1030 nm fluctuates periodically with 0.6 nm periodicity. This periodicity corresponds to the free spectral range of the Yb:YAG cavity. At a nominal input wavelength of 940 nm the output power fluctuates between 40 mW and 0 mW. Since the effect is related to the free spectral range of the Yb:YAG cavity, it would seem that the effect might be related to a wavelength dependent reflection of the Fabry Perot cavity set up between the input and output facet of the micro-laser array. Measurement of the reflectivity of the input facet and modeling of the reflection from the front facet as a function of wavelength showed that this effect is not sufficiently strong to explain the observed wavelength dependence of the micro-laser array.

II.2: COMPARISON WITH THEORY

To further understand our experimental results, we modeled the Yb:YAG cavity in collaboration with Dr. Jim Harisson at SEO. Using typical data for Yb:YAG in the literature,

we calculated the threshold pump power and slope efficiency for different configurations. The results of the calculation are summarized in Table 1. These calculations consider three different cases: (i) T.Y. Fan's experiment at MIT with a collimated laser diode source presented in column 1, (ii) SDL's experiment with Ti:Sapphire laser shown in column 2, and (iii) projection for a butt-coupled laser diode presented in column 3. The calculated threshold pump power for the SDL experiment with a Ti:Sapphire laser is 88 mW. A typical measured threshold value is 200 mW. T.Y Fan at MIT-LL has used beam shaping of the output from a 100 micron wide laser diode to focus the beam from the laser diode into a 75 by 90 micron spot. The experimental threshold pump current is 200 mW and the calculated threshold is 115 mW.

Yb:YAG Calculated Results			
Inputs	TY Fan	SDL Ti:S	SDL D-P
Pump Wavelength (nm)	940	940	940
Laser Wavelength (nm)	1030	1030	1030
Absorption Coeff. for Pump (cm-1)	19	10	19
Crystal Length (cm)	0.04	0.045	0.045
Ratio of Eff. Abs. Length to Crystal Length	2.00	2.00	2.00
Diameter of TEM100 Mode Inside Crystal (mm)	0.06	0.045	0.15
Diameter of Pump Mode Inside Crystal (mm)	0.09	0.056	0.15
Fractional RT Loss at Laser Wavelength	0.005	0.005	0.005
Output-Coupler Reflectivity (Fractional)	0.975	0.950	0.950
Effective Stim. Emission Cross Section (cm)	1.8E-20	1.8E-20	1.8E-20
UL Occ. Prob. @ Temp of Cross-Section Measurement	0.7	0.7	0.7
Upper State Lifetime (μsec)	1160	1160	1160
Dopant-Ion Density (cm-3)	3.5E+21	3.5E+21	3.5E+21
Lower-Level Occ. Probability	0.047	0.047	0.047
Upper-Level Occ. Probability	0.7	0.7	0.7
RT Ground-State Abs. (Fractional)	0.338	0.381	0.381
Pump Quantum Efficiency (%)	100	100	100
Crystal Index	1.82	1.82	1.82
% Excitation in Laser Upper Levels (co-doped)	100	100	100

Outputs	TY Fan	SDL Ti:S	SDL D-P
Ratio of Pump to Laser Beam Diameter	1.50	1.24	1.00
Fraction of Pump Absorbed(%)	78.1	59.3	81.9
Transmission: Pump-to-Crystal	0.90	0.80	0.90
Threshold Fluence at Crystal Face (W/cm^2)	1.8E+03	3.6E+03	2.8E+03
CW Threshold Power (mW)	114.23	88.26	495.59
Absorbed CW Threshold Power (mW)	80.32	41.90	365.36
Slope Efficiency (%)	53	39	61

Table 1: Summary of calculation of Yb:YAG micro-lasers.

For a simple butt-coupling scheme from a surface emitting laser array, the average spot size in the laser cavity is about 170 micron. Using simple micro-optics this may be somewhat reduced. As an example how the threshold pump power varies with the pump beam diameter, the third column in Table 1 shows the parameters and calculated results of a configuration where the pump beam from a laser diode is contained within a 150 micron spot size, such as for butt-coupling between laser diode and micro-laser array. The calculated threshold is approximately 500 mW with a slope efficiency of 61%. In a configuration where the light from a 2-D array of lasers is coupled to the microcavity, it is difficult to optimally shape the beam from all individual laser diodes in the array; and therefore the pump threshold for such a configuration will be similar to that for the butt-coupled configuration.

II.3. LASER DIODE PUMPING OF Yb:YAG

Based on the theoretical results discussed in the previous section it is clear that the pump threshold for laser diode pumping without beam shaping is relatively high, however using beam shaping the pump threshold may be reduced. In order to better understand what type of beam shaping would be required for optimal operation of the Yb:YAG cavity, we performed several experiments with laser diode pump sources. These experiments include the (i) fabrication of the laser diodes at 940 nm, (ii) beam shaping of the laser diode and imaging of the laser diode to a Yb:YAG micro cavity and (iii) butt-coupling of the laser diode to the Yb:YAG micro-laser. These experiments showed that although high power q-cw operation was obtained from the Yb:YAG micro-laser, no cw operation of Yb:YAG was obtained. The dependency of output power versus duty cycle was investigated. These investigations showed that the output power from the micro-laser is a strong function of duty cycle of the pump beam. The laser diode-pumped Yb:YAG experiments are described below in more detail.

II.3.1: Fabrication of 940 nm High Power Pump Lasers

High power laser diodes were fabricated with a wavelength of 940 nm. The laser diode is based on an epitaxial design with InGaAs strained quantum well. Instead of fabricating more complicated surface emitting laser arrays we fabricated simpler edge emitting laser arrays for our initial experiments. Figure 8a depicts a schematic diagram of the laser array. Each of the laser diodes is 100 micron wide and has a cavity length of 1 mm. The lasers are spaced on 600 micron centers with 8 elements on a bar. After cleaving and coating the laser bars are bonded on a passive Cu submount for cw operation. The Cu submount is mounted on a water cooled heat sink. Figure 8b-c summarizes the experimental results obtained from the edge-emitting laser array. Over 8 Watt cw output power was obtained from the 6 element array corresponding to over 1 Watt per element. The near field from the array shows a uniformity better than 20 % and the spectrum, is centered at around 940 nm. In addition to the laser array we also bonded several individual 100 micron wide broad area edge-emitting lasers. Figure 9 shows the measured output power versus input current for a single 100 micron wide laser diode bonded on a copper submount. Over 3 Watt output power was obtained at a wavelength of 941 nm.

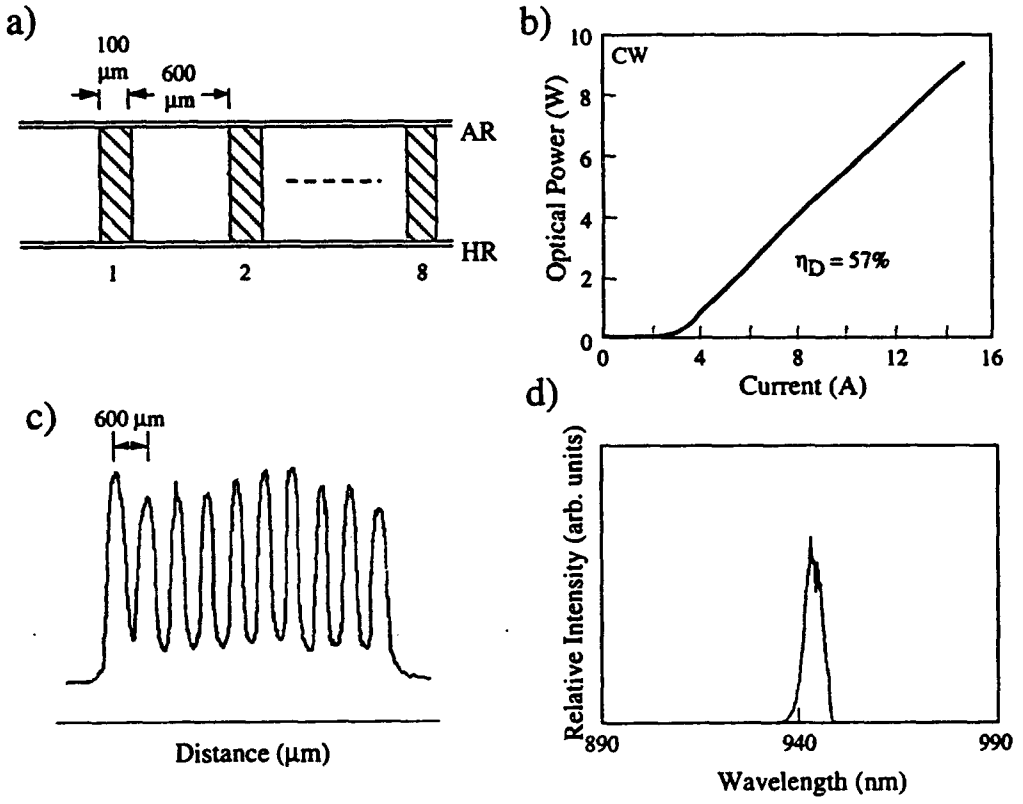

Figure 8: Summary of results of a 1-cm laser bar: a) schematic diagram, b) L-I, c) near field at 10 W, d) spectrum at 10 W.

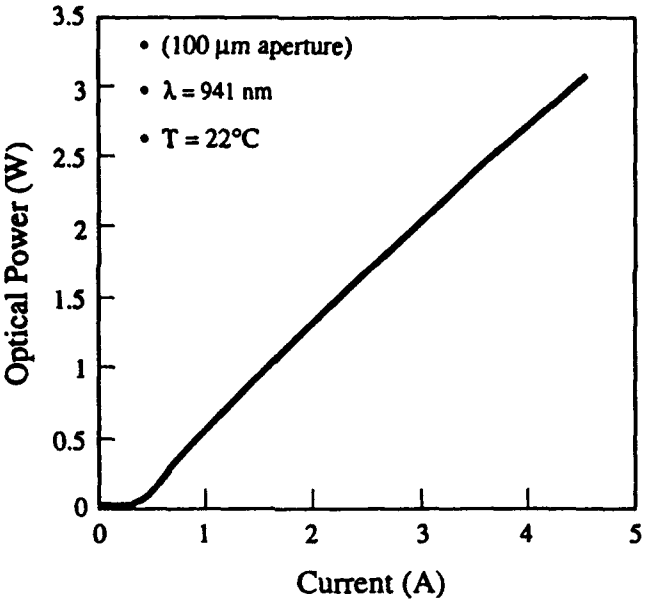

Figure 9: Light output versus input current for a single 100-μm wide edge-emitter.

II.3.2: Diode Pumping of Yb:YAG With Beam Shaping of the Laser Diodes

Initial experiments with laser diode pumping of the Yb:YAG laser used a single laser diode and beam shaping of the laser diode to optimize the pump spot size at the micro-laser. Figure 10 shows a schematic diagram of the experimental set up for beam shaping of the laser diode output from a single, 940 nm, 100 micron-wide laser diode. The output from the laser diode is collimated with an 8 mm focal length lens. In the direction parallel to the junction, a cylindrical telescope with 5 times magnification is used to symmetrize the beam from the laser diode. After symmetrization the beam is focused on the micro-laser with a 100 mm focal length lens. The measured focused spot size, shown in Figure 11, is approximately 20 μm by 40 μm in directions perpendicular and parallel to the junction, respectively. In the direction parallel the junction defocusing results in a change in the beam shape. The change in beam shape with defocusing is a result of the multi mode behavior of the light in the direction parallel to the junction. In the direction perpendicular to the junction the light from the laser diode is diffraction limited and the beam remains focused over the full length of the micro-laser crystal without changing shape.

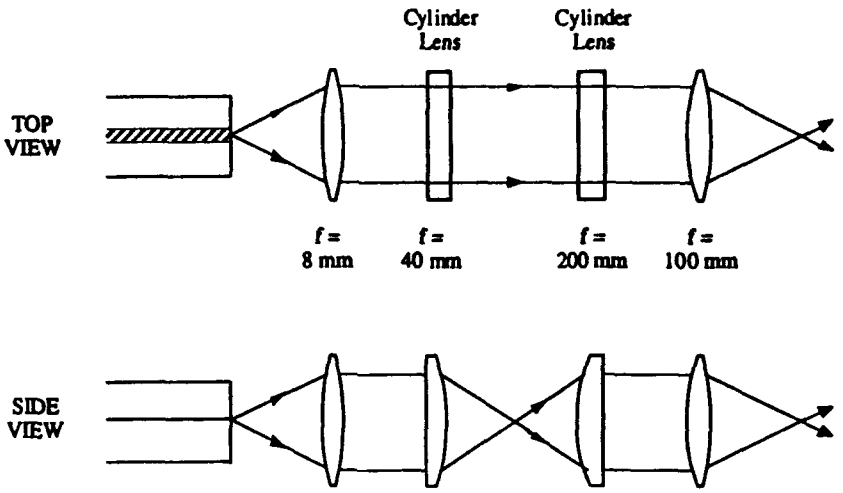

Figure 10: Schematic diagram of the experimental set-up to focus the light from a single 100-μm wide broad area laser to a Yb:YAG micro-laser.

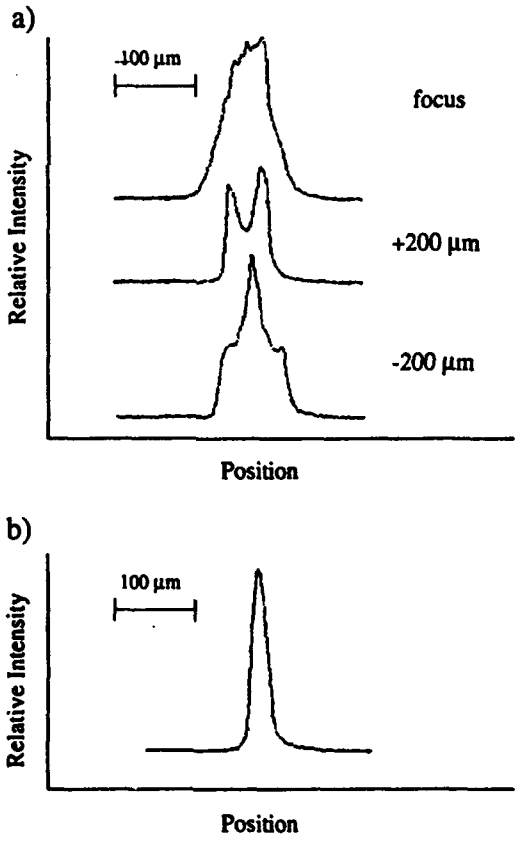

Figure 11: Measured focused spot of the pump beam at the Yb:YAG micro-laser: a) in direction parallel to laser junction, b) perpendicular to laser diode junction.

Initial experiments using cw operation of the laser diode up to 1-2 Watt and the 25 % doped Nd:YAG micro-laser showed a small flash at 1.03 μm wavelength when the laser diode was turned on; however no sustained laser operation was achieved. Therefore the laser diode was operated in a q-cw mode. Figure 12, shows the measured output power from the micro-laser at a wavelength of 1.03 micron as a function of the pump power. The threshold pump power is 400 mW and a maximum output power of 11 mW was achieved at an input power of 1.5 Watt. The operating conditions were 40 Hz and 1. 7 ms pulse width, which results in a duty cycle of 7 %. The measured optical-to-optical slope efficiency is 8 %.

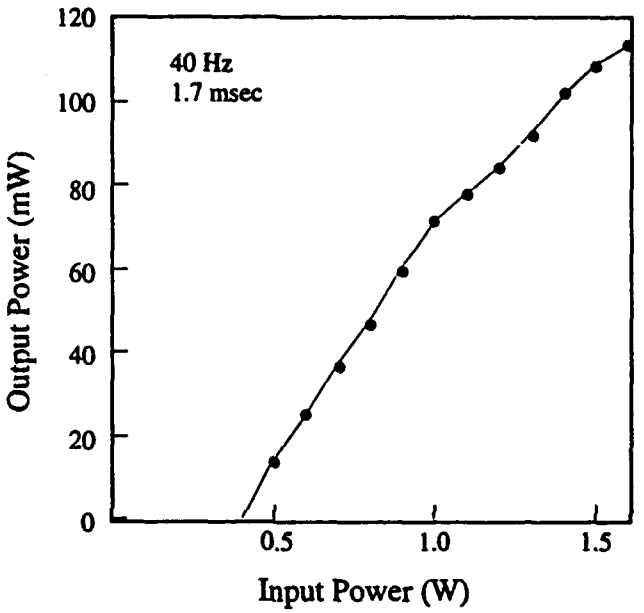

Figure 12: Measured output power versus input pump power from a Yb:YAG micro-laser pumped with a single laser diode. An imaging system (shown in Figure 10) was used to shape the beam from the laser diode.

We further investigated why the micro-laser does not operate under cw operation by changing the duty cycle of the pump light. Figure 13 shows the measured relative output power from the Yb:YAG laser as a function of pulse length. As the duty cycle is increased by changing the pulse width of the pump beam while the repetition rate remains constant, the relatively output intensity from the Yb:YAG micro-laser decreases rapidly. For approximately 50% duty cycle the output power is nearly zero. Figure 14 shows the experimental results obtained when the duty cycle of the pump beam is changed by increasing the repetition rate of the pump light for a constant pump pulse width of 1 msec. The output power is again decreased with duty cycle. Based on the experiments with varying duty cycle, it is clear that the efficiency of the micro-laser depends on the average duty cycle of the pump beam. This seems to indicate that thermal effects are the cause of the reduction of output power under cw operation. Since the Yb:YAG is a quasi three level system, the operation of the micro-laser depends on the temperature much more strongly as compared to

a four level system such as Nd:YAG lasing at 1.06 micron. However, the observed dependency on duty cycle is stronger than expected. We have compared our results with the experimental results obtained from researchers from MIT-LL and Aerospace. The Aerospace results confirm our experimental finding, however the MIT-LL results show cw operation with laser diode pumping. In all experiments the same material was used from the same vendor.

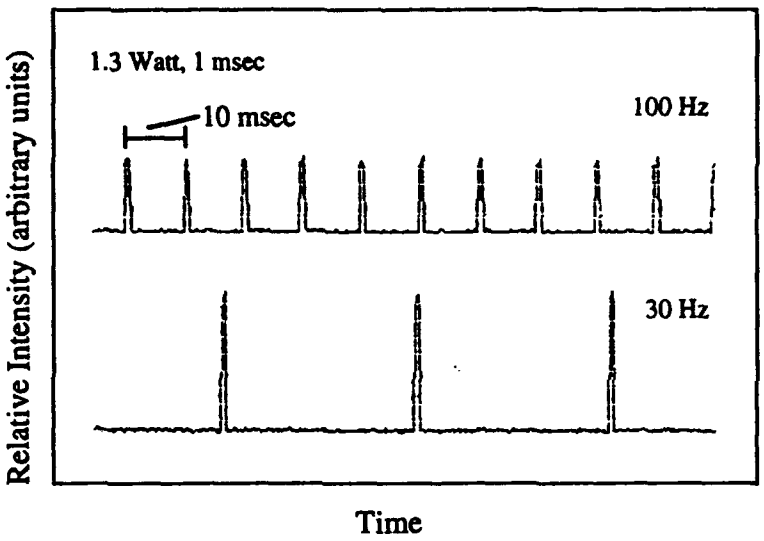

Figure 13: Relative output power as a function of duty cycle for a Yb:YAG micro-laser.

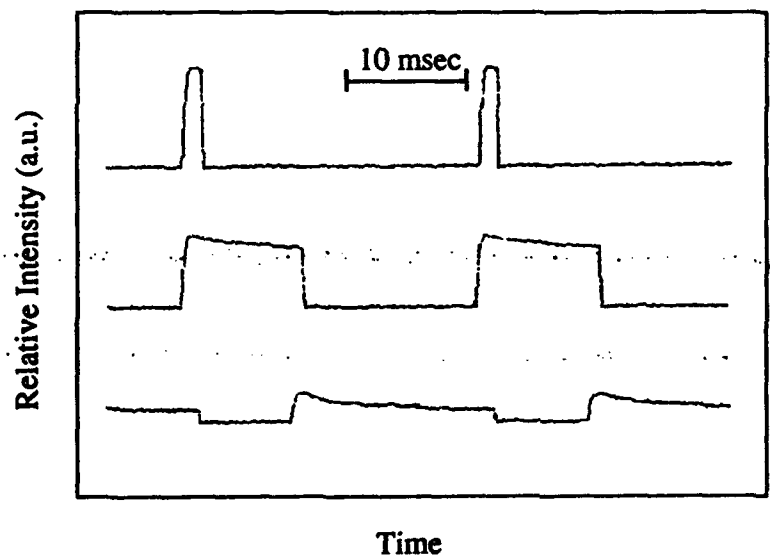

Figure 14: Reflective output power at 1.03 μm as a function of time for different pulse lengths.

In a final experiment with laser diode pumping of Yb:YAG, the performance of a butt coupled Yb:YAG laser was investigated. A single 100 micron wide laser diode similar to the laser diode used in the previously described experiments is used to pump the 25 % doped Yb:YAG micro-laser using a butt-coupled configuration. Figure 15 shows the measured output power as a function of input pump power for different separation between the laser diode and the input facet of the micro-laser. The operating conditions of the laser diode pump are 1 msec pulse length and 40 Hz. For the smallest spacing between the laser diode and the micro-laser, 20 micron, the threshold pump power is measured to be 650 mW and a maximum peak output power of 200 mW is obtained at an input power of 1.7 Watt. For larger separation between the laser diode and the micro-laser, the pump threshold increases while the slope efficiency remains approximately constant. This means that if the Yb:YAG micro-laser is used in conjunction with a 2-D surface emitting laser array, we can expect over 50 mW output power per element based on 1 Watt input power per element, however the efficiency is relatively low and no cw operation is demonstrated. Partly because of these limitations, the developments of Yb:YAG micro-lasers was not further pursued. Instead, the research was focused on the development of Er:YSGG micro-lasers which are discussion in the subsequent sections of this report.

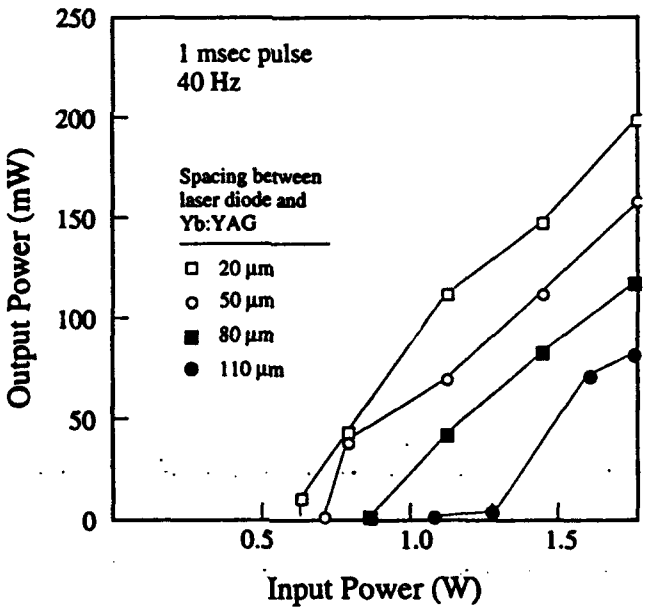

Figure 15: Measured output power from a Yb:YAG micro-laser, butt-coupled to a single 100-μm wide laser diode. The parameter is the distance between the laser diode and the Yb:YAG micro-laser.

III: EXPERIMENTAL RESULTS LINEAR ER:YSGG MICRO-LASER ARRAY

In this section the results obtained with a linear array of Er:YSGG micro-lasers pumped with a linear edge-emitting laser diode bar are discussed. Based on the results obtained with the linear micro-laser array, a monolithic 2-D surface-emitting laser array has been developed which is discussed in Section IV. The results obtained with a 2-D Er:YSGG micro-laser array are discussed in Section V.

Er:YSGG is pumped at around 970 nm and has a laser transition at 2.8 micron. The insert in Figure 16 shows a partial energy diagram for Er:YSGG. The 970 nm pump beam excites the atom to the $4_{I11/2}$ state. The 2.8 micron laser transition is between the $4_{I11/2}$ state and the $4_{I13/2}$ state. The $4_{I13/2}$ lower level has a relatively long lifetime which would make this laser transition inefficient. However, fortunately, there is a second pump mechanism in Er:YSGG in which the $4_{I13/2}$ level is depopulated through an upconversion process. Moreover, part of the unconverted states relax back to the $4_{I11/2}$ level, such that this energy can again contribute to the 2.8 micron lasing transition. The net effect of the pumping mechanism is that the quantum efficiency of this system may be higher than the quantum efficiency based on the energy difference between the pump light and the laser transition. Comparison of Er^{3+} in different hosts has shown that the YSGG host is more efficient as compared to other hosts such as YAG.[11] The measured absorption coefficient of Er:YSGG as a function of wavelength and the measured lasing output power as a function of pump wavelength as shown in Figure 16. The pump absorption spectrum exhibits several narrow peaks at around 965 nm and some additional smaller peaks at around 970 nm. On the other hand, the measured output power at 2.8 micron from an Er:YSGG laser as a function of pump wavelength (excitation spectrum) shows a wide wavelength band of the pump laser ranging from 960 nm to 980 nm with high output power. The excitation spectrum is much wider than the absorption spectrum because of the high pump density. At 200 mW pump power, the micro-laser is operating about 30X above threshold. The broad pump spectrum is advantageous for actual diode-pumped systems. In such systems the bandwidth of the individual laser diodes may be several nm or wider and for 2-D arrays the wavelength may vary over the array.

Er:YSGG micro-lasers were provided by SEO. The micro-lasers have a thickness of 1 mm and dielectric reflectors deposited directly on micro-laser facets. The input reflector has high transmission at the 970 nm pump wavelength and over 99 % reflection at the 2.8 micron lasing wavelength. The reflection of the output facet of the micro-laser is 95 % at the lasing wavelength for output coupling of the light at 2.8 micron. The output reflector also reflects back part of the pump wavelength for more efficient absorption of the pump beam. The SEO micro-lasers, which were developed under an ARPA contract were made available to the SDL ARPA program with permission of the sponsor.

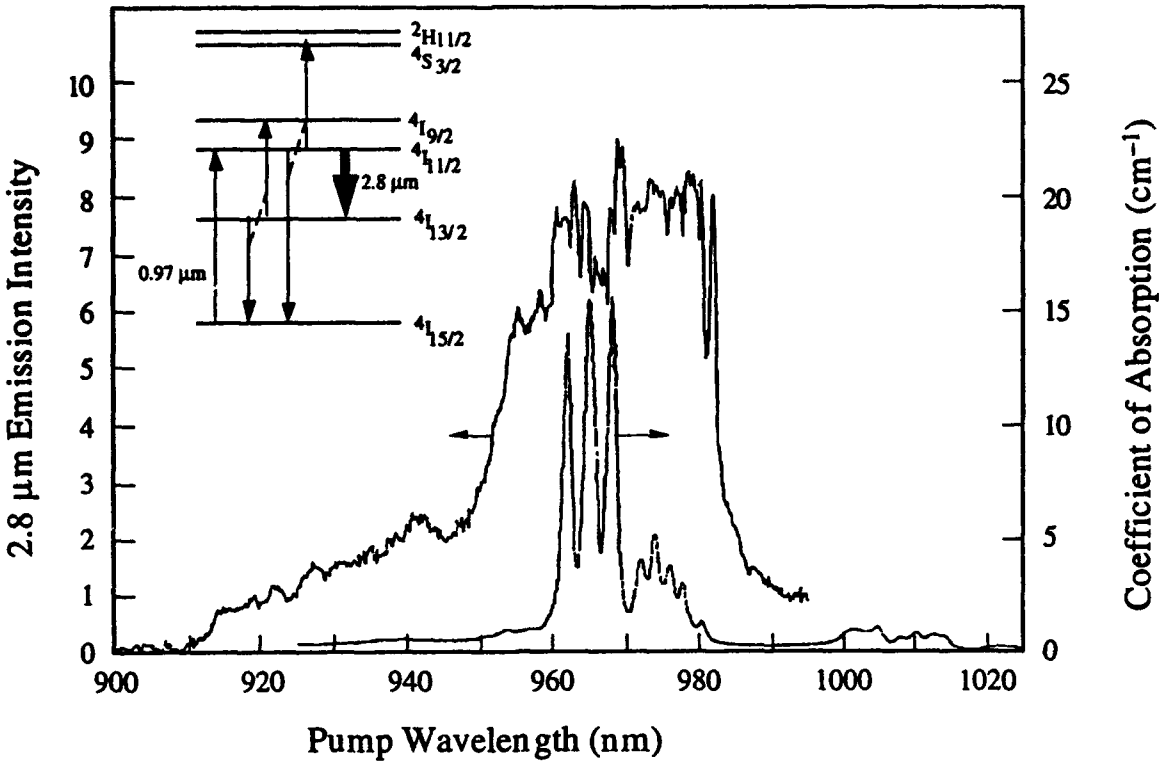

Figure 16: Absorption and emission spectrum of Er:YSGG. The insert show a partial energy diagram.

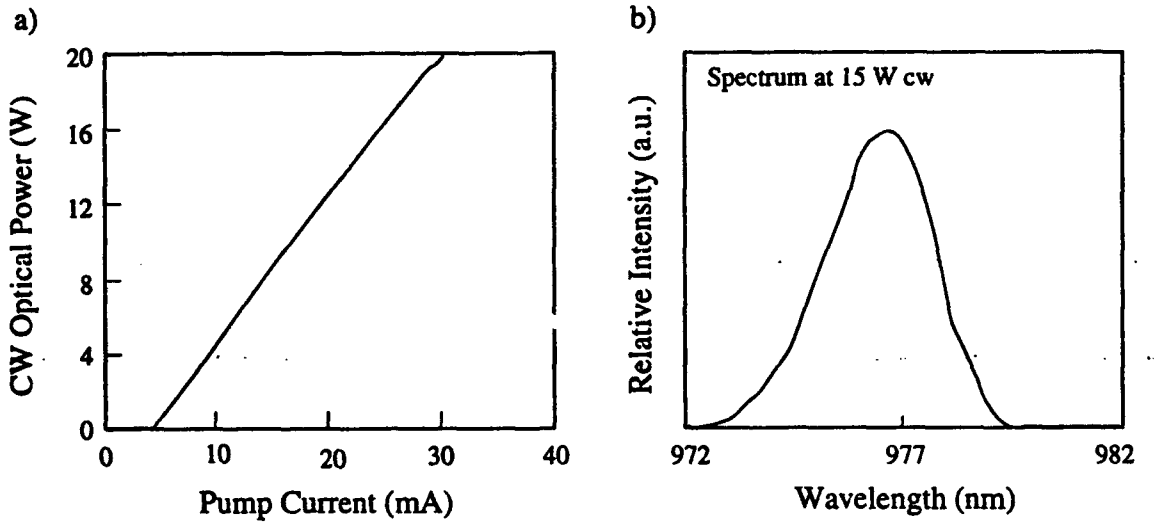

Figure 17: Summary of the experimental results from a 12-element 1-cm long laser diode bar.

Initial experiments with the Er:YSGG micro-laser were performed using a linear laser diode bar. The experiments were performed in collaboration between personnel of SDL and SEO. A 15 Watt cw (SDL 3450-S) laser bar is used as a pump source. Figure 17 summarizes the measurement characteristics of the laser diode bar. A maximum 20 Watt cw output power is obtained from the 1 cm laser diode bar at a pump current of 30 Amps. The spectrum of the bar at room temperature is centered around 977 nm with a width of 2 nm FWHM. Several optical coupling schemes were investigated for coupling the optical output from the laser diode bar to the Er:YSGG. A schematic diagram of the three different configurations is shown in Figure 18. Figure 18a depicts the most simple coupling scheme with the laser diode bar directly butt-coupled to the micro-laser. The distance between the laser diode and the micro-laser can be varied. Figure 18b shows an optical coupling scheme with a fiber lens for collimation of the light in the direction perpendicular to the junction. Finally, in Figure 18c the light from the laser diode bar is collimated with the same fiber lens as in Figure 18b, however, this fiber lens is followed by a microlens array which focuses the light from each laser in the laser diode array onto the microchip. More details on the optical coupling scheme together with a detailed analysis of the mode shape of the micro-laser and its effect on micro-laser efficiency are presented in a report presented to ARPA by SEO and a related paper.[11] The efficiency of the micro-laser is determined by the overlap between the pump beam and the cavity mode. The cavity mode is determined by the thermally induced index changes and bowing of the reflectors at the surface of the micro-laser. By using micro-optics to shape the beam from the laser diode, the pump intensity is increased and the pump threshold is reduced, resulting in a higher total efficiency of the micro-laser.

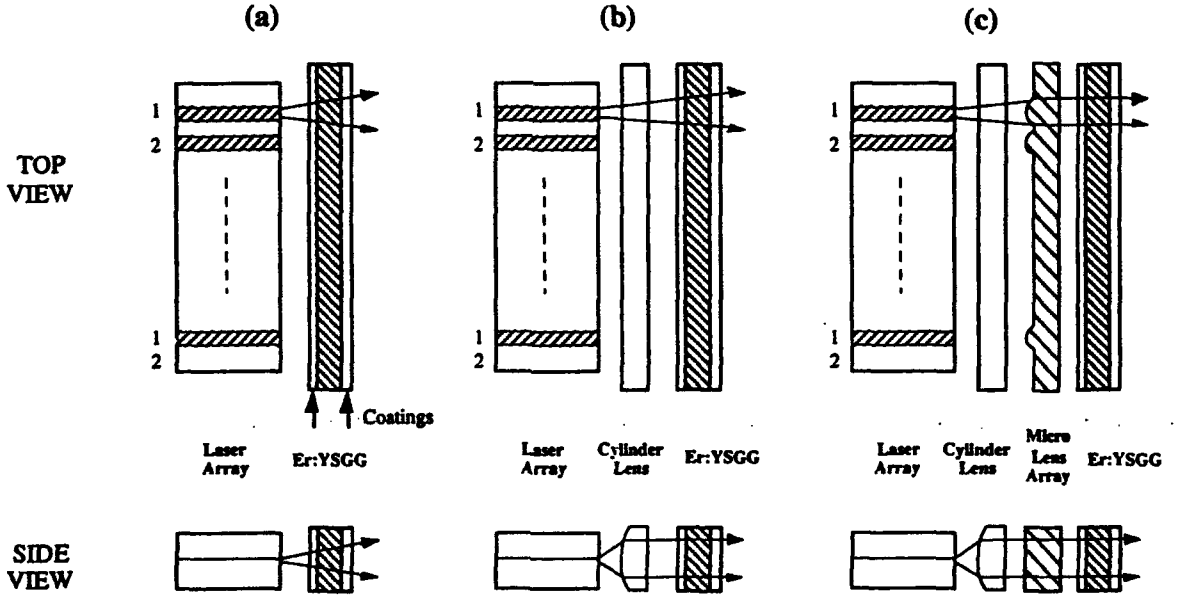

Figure 18: Schematic diagram of the experimental set-up with a linear laser diode array coupled to an Er:YSGG micro-laser: a) no coupling optics, b) cylinder lens as coupling optics, c) cylinder lens and micro-lens as coupling optics.

The first series of experiments was based on the cylinder lens and microlens array shown in Figure 18c. The optimal wavelength of the laser diode pump was determined by varying the operating temperature of the laser diode array mounted on a water-cooled heat sink. Figure 19 shows the measured output power at 2.8 micron wavelength as a function of pump wavelength. The optimal output power was obtained at a 973 nm wavelength of the pump laser. All subsequent experiments with the linear laser array were performed at this wavelength.

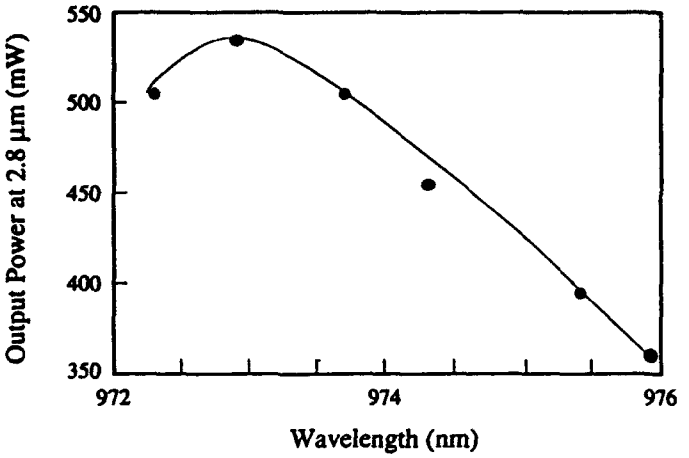

Figure 19: Measured output power at 2.8 μm as a function of the center wavelength of the laser diode bar.

Figure 20 shows the measured output power at 2.8 micron as a function of pump power for the three different configurations shown in Figure 18. Using a fiber cylinder lens and micro lens a maximum output power of 930 mW was demonstrated at 15 Watt total pump power. Without the micro lens the maximum output power at 15 Watt pump power is 700 mW and using direct butt-coupling the output power is reduced to 450 mW. In the butt-coupling scheme the laser diode was approximately 50 micron distance from the micro-laser in order to obtain the best efficiency and output power. The close proximity of the laser diode to the micro-laser results in very high local power density of the laser diode light at the micro-laser. As a result of the high power density, the microchip fractured at 15 Watt optical input power.

The output beam quality of the micro-laser array was investigated with the experimental set up shown in Figure 21. The output from the Er:YSGG micro-laser array is filtered to block the pump light at around 970 nm and a CaF_2 lens with high transmission at around 3 micron wavelength is used to form a far field of the array at the focal plane of the lens. A Sphericon linear thermopile array was used to measure the intensity distribution at the focal plane of the lens. The experimental results of the far field measurements are shown in Figure 22. In the vertical direction, perpendicular to the plane of the laser diode junction, the light from the array is near diffraction limited with a divergence of 0.48° at a pump power of 6 Watts. For higher pump power the far field of the array shows a slight broadening. This broadening may

be caused either by a change in the mode size in the micro-laser due to a difference in the thermal effects, or alternatively may be a result of the lasing of higher order modes. Based on the measured shape of the beam, which is close to that of a lowest order Gaussian beam, it is more likely that a change in mode size has occurred. In the horizontal direction, the far field is wider than the vertical direction. A possible reason for this wider far field is that the twelve beams do not all steer in the same direction.

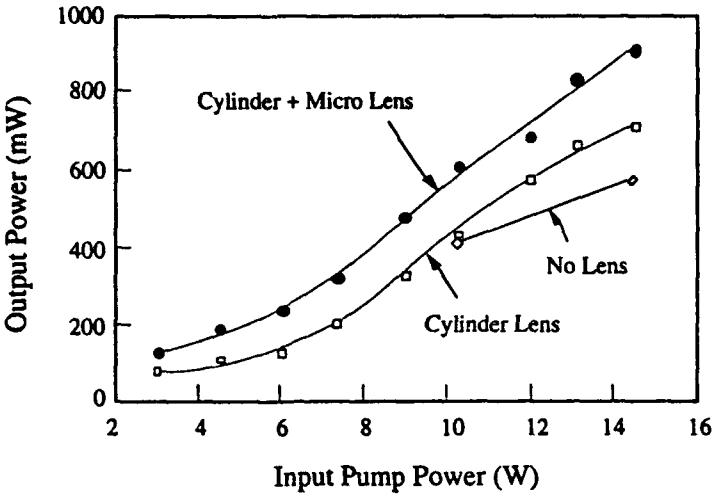

Figure 20: Measured output power at 2.8 μm from the Er:YSGG micro-laser pumped with a 1-cm, 12-element laser diode bar. The parameter is the optical coupling configuration between the laser diode bar and the Er:YSGG cavity.

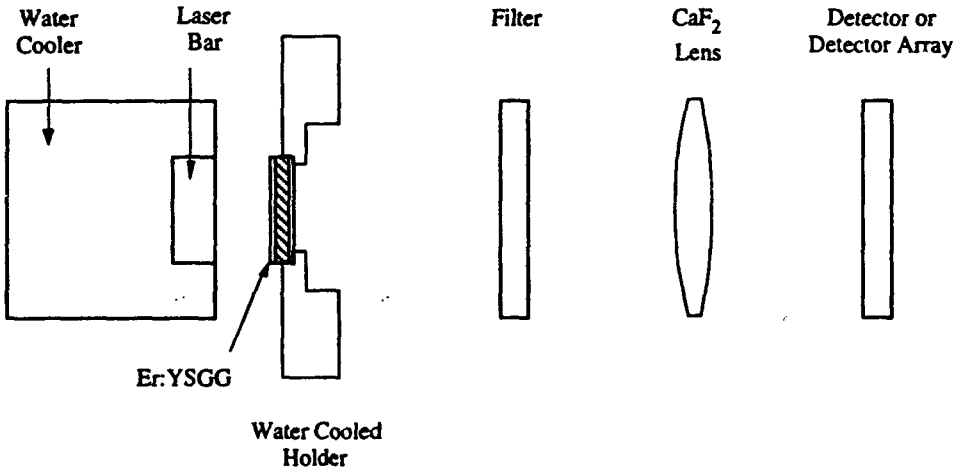

Figure 21: Schematic diagram of the experimental set-up to measure the far field from the Er:YSGG micro-laser.

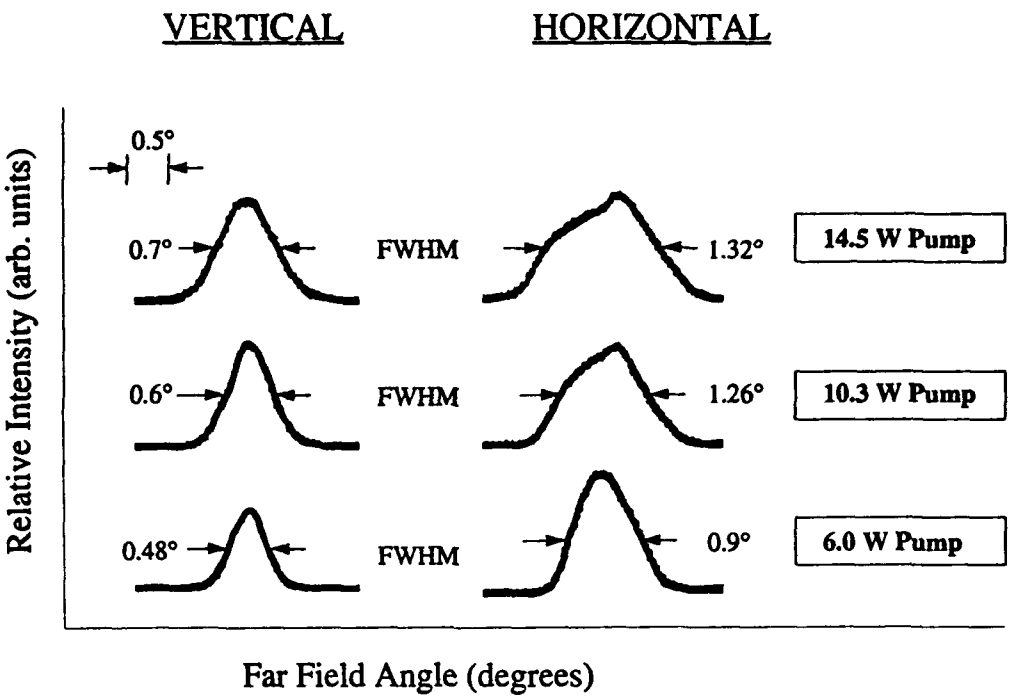

Figure 22: Measured far field from the Er:YSGG, 12-element micro-laser as a function of pump power.

For the 2-D micro-laser cavity, no special micro-optic is available to shape the optical output from the 2-D laser diode. Therefore the 2-D array is based on butt-coupling of the laser diode array to the micro-laser array. We further measured the performance of the butt-coupled linear laser diode array to the micro-laser by measuring the output power from the micro-laser as a function of the distance between the laser diode array and the input facet of the micro-laser array. Figure 23 shows the experimental results. As can be seen from this Figure, the efficiency of the butt-coupled micro-laser array decreases as a function of the space between the laser diode array and the micro-laser. For a typical 2-D micro-laser array, the light from the diode array is coupled out through the GaAs substrate which has a typical thickness of 200 micron. Taking into account the index of GaAs of 3.5, this results in an effective optical distance between the laser diode and micro-laser input facet of approximately 60 micron.

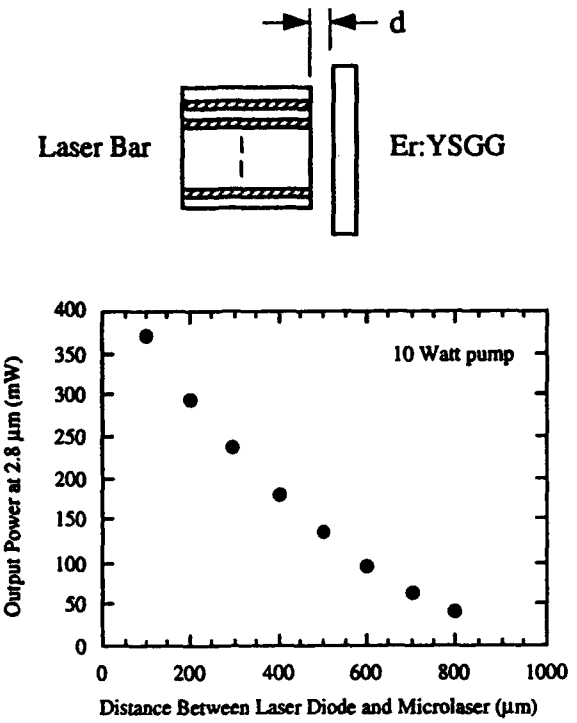

Figure 23: Measured output power at 2.8 µm from the Er:YSGG micro-laser butt-coupled to a 1-cm, 12-element laser diode array as a function of the distance between the pump laser and the Er:YSGG micro-laser.

IV. DEVELOPMENT 2-D LASER ARRAYS

Monolithic 2-D arrays can be used in high-power applications such as pumps for solid state lasers and possible hybrid 2-D pump source (stacked bars) replacements. The two basic approaches to fabricate 2-D surface-emitting laser (SEL) arrays are vertical cavity designs and horizontal cavities with etched beam reflectors. The horizontal cavity SEL with etched 45° reflectors has been more successful in obtaining high power per element as well as high total output power. In this section, we describe the fabrication and operation of high power monolithic 2-D SEL arrays. We have achieved 3.4 W cw and greater than 130 W q-cw power from a single element and a monolithic 4 x 12-element array of 150 μm wide surface emitter lasers with ion milled facets, respectively.

The two basic configurations of the SEL array are presented in a schematic form in Figs. 24 and 25. A single element SEL consists of a 150 μm x 1000 μm gain-guided InGaAs gain cavity and 90° and 45° reflectors. The 90° and 45° facets are etched to a 3.5 μm depth using Ar^+ ion mill. The 90° facet is coated with a high reflectivity coating (R approximately 85 %). The light in the gain cavity undergoes total internal reflection at the 45° facet. Two possible configurations for surface emitting lasers were investigated. In the first configuration shown schematically in Figure 24a, the optical feedback is provide by a short DBR grating fabricated in the device just before the 45° mirror. The second configuration shown in Figure 24b has a *build in superlattice reflector* which is positioned a few microns above the 45° mirror and reflects back approximately 5% of the light. The roughness of the ion milled facet has been measured to be as low as 10 nm RMS using an optical microscope interferometer. The smoothness of the etched facet is critical in reducing scattering and absorption at the facet that reduces the performance and the reliability of lasers with etched facets.

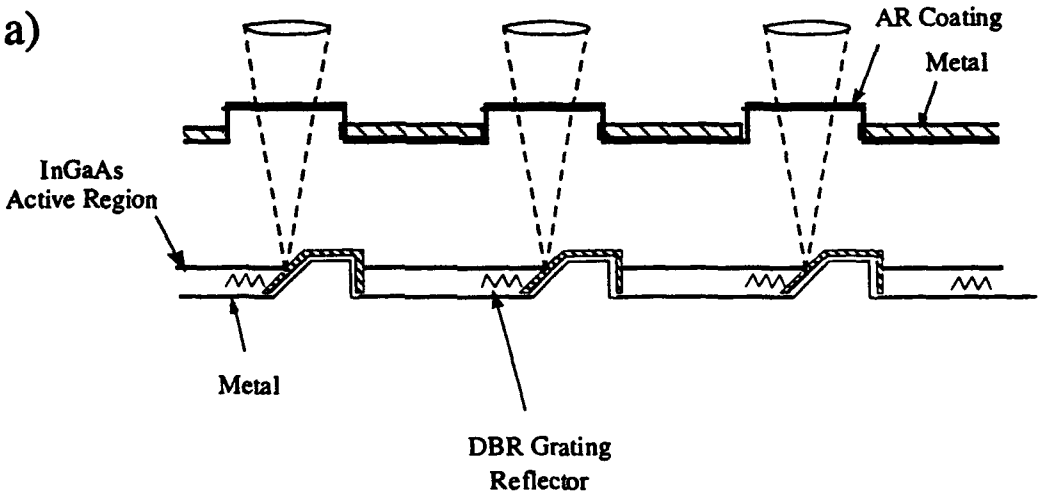

b)

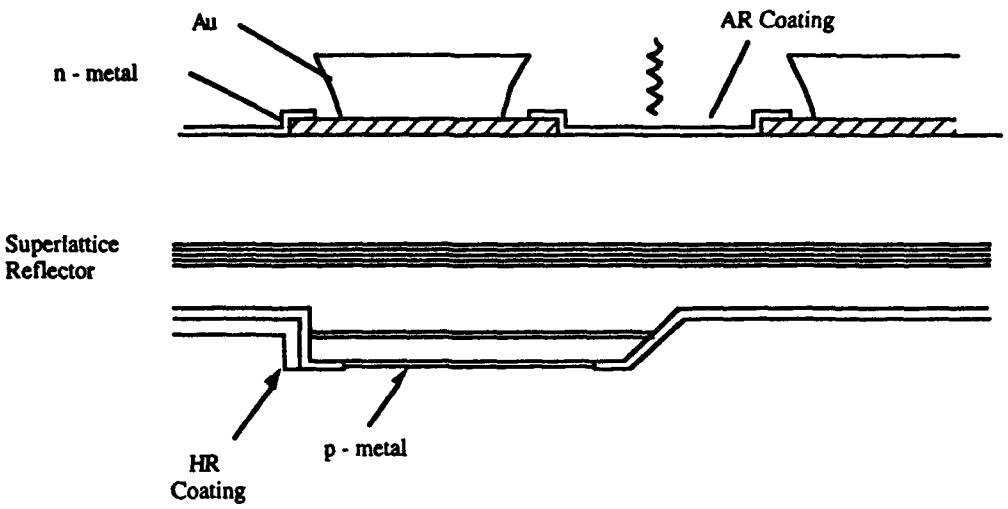

Figure 24: Schematic diagram of the surface-emitting laser diodes, a) with grating for feedback, b) with superlattice reflector for feedback.

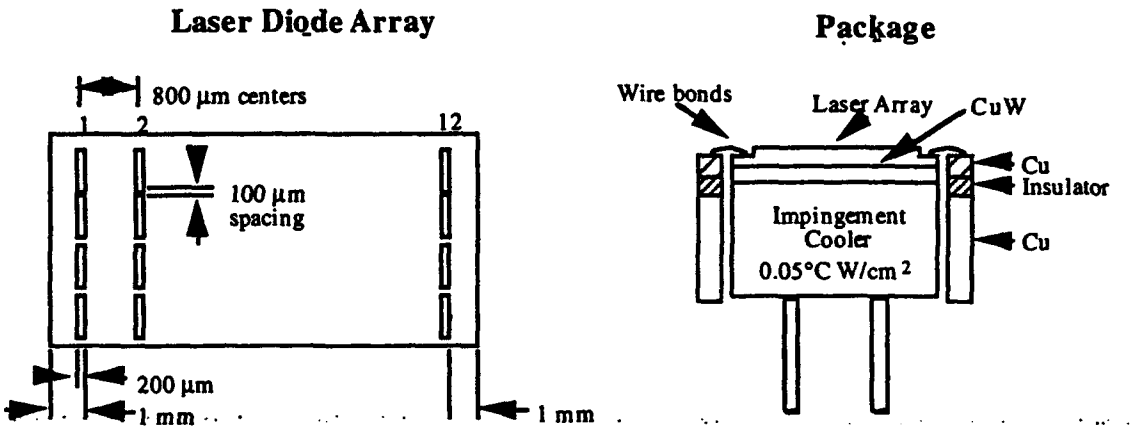

Figure 25: Schematic diagram of the 2-D surface-emitting laser diode array.

The horizontal gain cavity consists of single $In_xGa_{1-x}As$-$Al_xGa_{1-x}As$ quantum well heterostructure (QWH) grown via metalorganic chemical vapor deposition (MOCVD) that is designed to emit light at a wavelength of 970 nm through the n-type GaAs substrate. Figure 26 shows the epitaxial layers of the $In_xGa_{1-x}As$-$Al_xGa_{1-x}As$ QWH. The QWH consists of, starting from the GaAs substrate, (1) an n-type $Al_{0.4}Ga_{0.6}As$ lower cladding layer, (2) an n-type $Al_{0.3}Ga_{0.7}As$ lower and a symmetric p-type upper confinement layers with an $In_{0.2}Ga_{0.8}As$ quantum well at the center, (3) a p-type $Al_{0.4}Ga_{0.6}As$ upper cladding layer and (4) p^+-type GaAs contact layer.

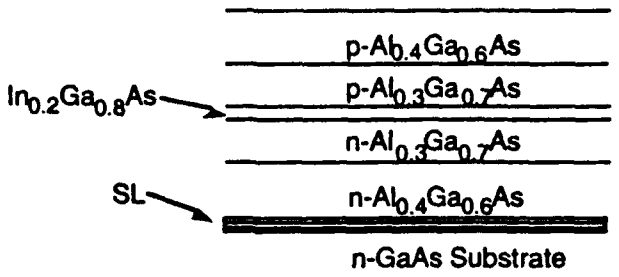

Figure 26: Epitaxial structure of the 970 nm surface-emitting laser diodes.

We first discuss the results obtained with the feedback for laser operation provided by a five period 1/4 λ $Al_{0.6}Ga_{0.4}As$-$Al_{0.2}Ga_{0.8}As$ superlattice reflector designed for ~5 % reflectivity and located 2 μm below the active region. A shallow proton bombardment is used to define 150 μm wide stripes on 750 μm centers. The length of the gain cavity is 1000 μm. The lasers are on 1150 μm centers in the direction along the length of the cavity. The GaAs substrate is polished to 200 μm thickness and coated with an anti-reflective layer for light output through the substrate. The surface emitter is metallized on n- and p- sides. Finally, a 20-25 μm of Au is selectively electroplated onto the n-side of the 2-D array for uniform current spreading and reduced contact resistance.

For initial characterization, single element surface emitter lasers are cleaved from the finished laser diode arrays and bonded p-down on Cu heatsinks, and tested. The cw light *output versus current* characteristics of a typical single-element 150 μm wide surface-emitting laser is presented in Fig. 27. A cw threshold current of 500 mA (Jth = 330 A/cm^2) and a differential efficiency of 47 % (0.6 W/A) are measured until heating effects cause the efficiency of the device to decrease. In addition, 3.4 W cw output power is obtained from the laser diode at 973 nm wavelength. The spectral characteristic of the laser diode is shown in the inset of Fig. 27. [The output power achieved from the laser diode is comparable to that of commercially available Fabry-Perot broad area lasers (1-3 W).] The full-width at half maximum (FWHM) of the perpendicular far field is measured as 28°.

Monolithic 2-D laser diode arrays consisting of 4 x12 elements (0.5 cm x 1 cm) were bonded p-side down (junction side) on an impingement type water-cooled cu heat sink for array characterization. The initial temperature of the 2-D SEL array measured at the top of the device is 20° C and the thermal resistance of the heat sink is 0.10° C/W. The q-cw L-I characteristic of the 4 x 12 element laser diode array is presented in Fig. 28. The pulse width and repetition rate of the current supply are 100 μs and 50 Hz, respectively. The q-cw threshold of the SEL array is 22.5 A (470 mA/device). A differential quantum efficiency of 47 % is obtained before the onset of a slight thermal rollover. A total peak output power of 132 W Q-CW (2.75 W/element) is achieved from the 2-D array which corresponds to an optical power density of 264 W/cm^2. The total power output from the 4 x 12 SEL array is limited by the current supply. The peak of the 2-D SEL array spectral output is at 973 nm with FWHM of 7.5 nm. These result represents the highest optical power and the highest optical power density from a surface emitting laser array.

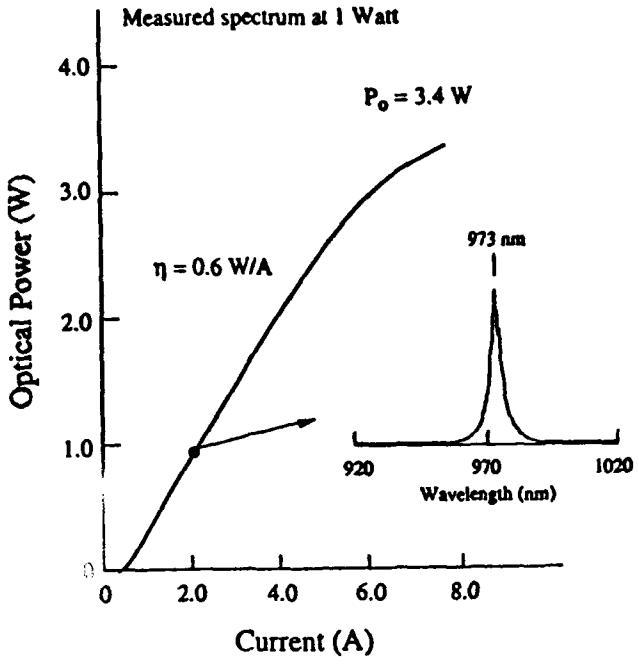

Figure 27: Measured output power versus input current for a single element 200 μm surface-emitting laser with superlattice reflector.

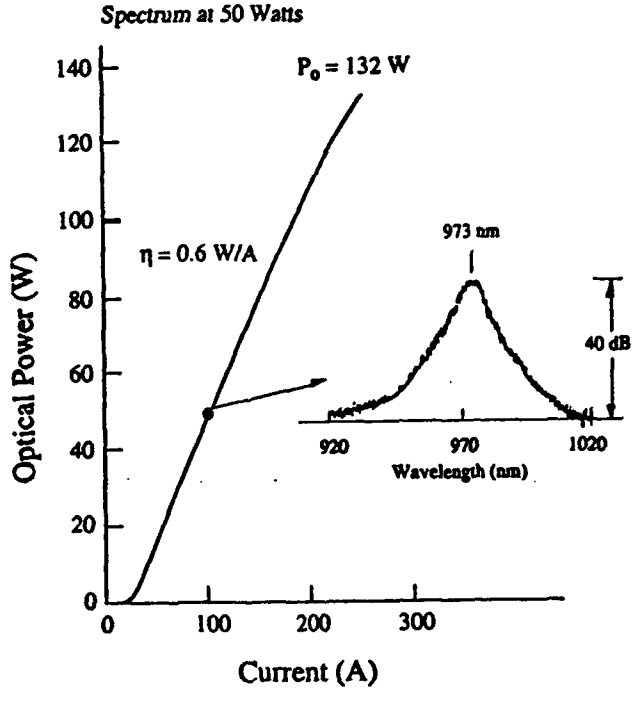

Figure 28: Measured output power versus input current from a 12 x 4 element surface-emitting laser array. The laser operates QCW (100 μsec pulse width, 50 Hz).

The near field of the 2-D array obtained at 100 A pump current is shown in Fig. 29. The near field shows good uniform intensity distribution across the entire 4 x 12 array. This uniformity is the direct result of the monolithic processing of 2-D arrays and an even distribution of current attributed to the uniform bonding and the thick Au plating. The high output power, spectral output, and good uniform characteristics of the 2-D SEL array make this array an excellent choice as the pump for Er doped YSGG in a micro-laser configuration.

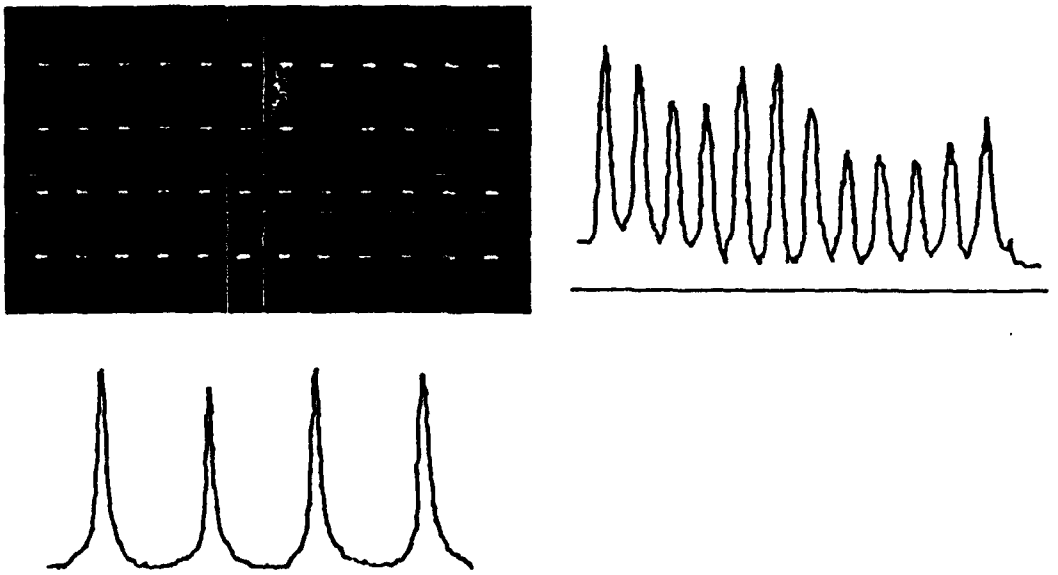

Figure 29: Measured near field of the 12 x 4 element surface-emitting laser array. The spacing is 750 μm and 1100 μm in the horizontal and vertical directions respectively. Operating conditions are QCW (210 μsec pulse width, 104 Hz, I=100A).

In addition to the 2-D surface emitting laser array with superlattice reflectors (Fig. 24b), 2-D surface-emitting laser arrays were fabricated with distributed Bragg reflectors (DBRs) as shown in Figure 24a. The epitaxial layers are grown by a two-step metal-organic chemical vapor deposition (MOCVD) process. The first growth consists of the n-type AlGaAs lower confining layer, the AlGaAs waveguide core and active region, and ~0.2 μm of the p-type AlGaAs confining layer. The active region of the device is composed of InGaAs quantum wells. Following the growth, the gain regions are patterned using photolithographic techniques. A thin photoresist is spun onto the wafer and exposed using holographic techniques. After developing, the sample is etched to form the grating in the epitaxial layers. The gain regions are not etched. The wafer is then cleaned and prepared for MOCVD regrowth. The second MOCVD growth finishes the p-type upper confining layer and provides a p-doped GaAs layer for ohmic contact purposes. The length of the DBR section of the surface emitting laser is 30 μm. No superlattice reflector structure is grown during the initial epitaxial growth for the DBR surface emitting lasers. The subsequent processing steps

and resulting device dimensions for the DBR surface emitting lasers are identical to the superlattice surface emitting lasers described above.

The critical fabrication step of the DBR lasers is the relative positions with respect to wavelength of the peak of the DBR reflectivity and the gain peak of the laser epitaxial structures. A small detuning (3-5 nm) of the DBR peak from the gain peak can result in a drastic reduction in efficiency and increase in laser threshold. During this program, we fabricated and characterized several DBR surface emitting lasers. The wavelength of the DBR grating was chosen according the photoluminescence (PL) peak of the laser structure. In most cases, however, the DBR surface emitting lasers operated at high threshold currents and low slope efficiencies indicating a poor overlap between the gain peak of the InGaAs laser structure and the peak of the DBR reflectivity.

We were able to operate some of the DBR surface emitting laser diodes with high efficiency and low threshold as shown in Figure 30. The single 200 μm-wide DBR incorporated surface emitting laser operated up to 2.4 W cw with a threshold current of 0.5 A and a differential slope efficiency of $\eta \approx 45\%$. The wavelength of the surface emitting laser was centered at 964.5 nm with a FWHM of nearly 4-5 nm. The narrow spectrum and slow temperature tuning versus wavelength characteristics of DBR lasers (≈0.06 nm/°C) were not evident in the spectral output of the DBR surface emitting lasers. In addition, the peak wavelength of the surface emitting laser was nearly 10 nm shorter than the designed peak of the DBR reflectivity. We speculate that the reflectivity peak of the DBR grating was too far away from the gain peak of the lasers thus the surface emitting lasers operate without being affected by the feedback from the DBR. We did not use the DBR surface emitting laser arrays to pump the Er:YSGG since these devices have lower output power as compared to the superlattice surface-emitting devices and in addition the peak output wavelength is approximately 8 nm shorter than the optimal pump wavelength.

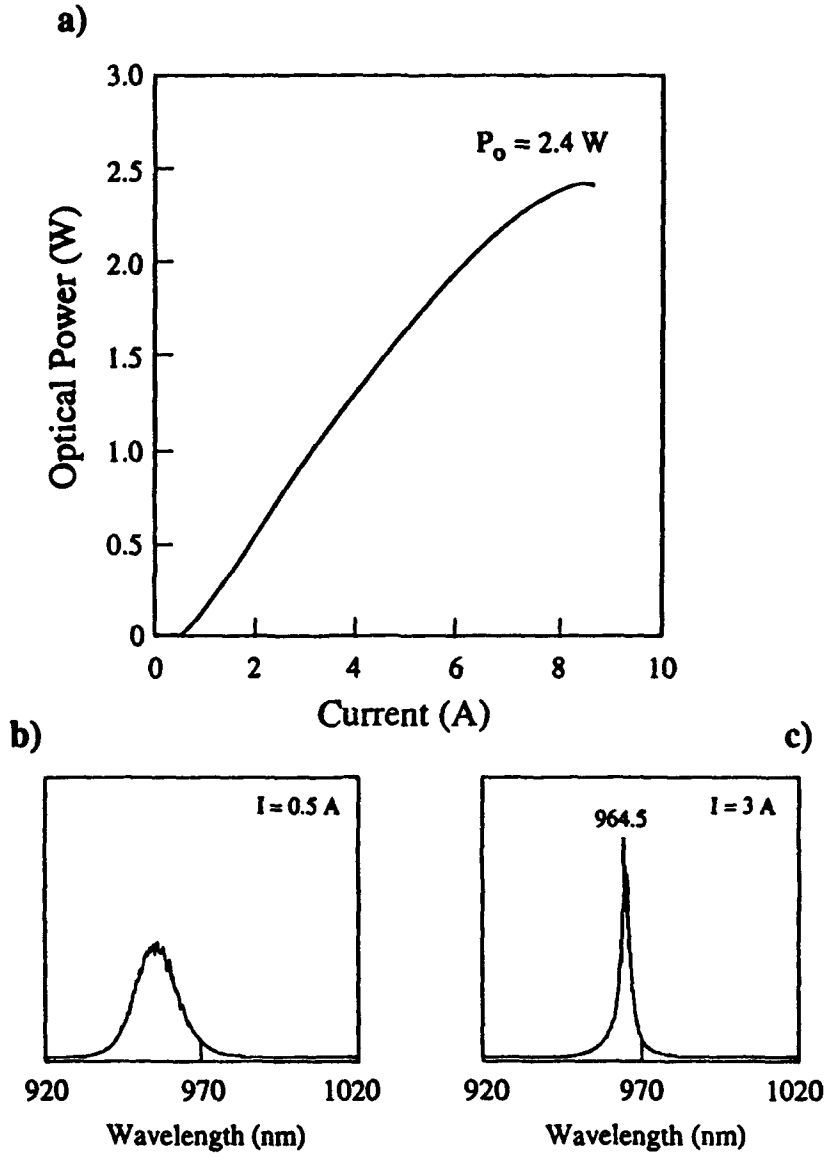

Figure 30: Summary of measurements from a 150-μm wide surface-emitting laser with DBR feedback: a) L-I, b) spectrum at 0.5 A, c) spectrum at 3A.

V. DEMONSTRATION 2-D Er:YSGG MICRO-LASER ARRAY

The 2-D laser diode array, with the experimental results presented in Figures 28 and 29, was butt-coupled to an Er:YSGG laser array similar to the array used in the experiments with the linear laser diode array. The size or the microchip matches the total aperture of the laser diode array and the micro-laser is bonded to a water cooled copper heat sink . The laser diode array was operated q-cw with a 5 msec pulse length and 5 Hz repetition rate. Figure 31 presents the measured output power at 2.8 micron versus the pump power from the 2-D laser array. A maximum output power of 600 mW (12.5 mW/element) was demonstrated at 42 Watt input power. The measured pump threshold power is approximately 20 Watt. Based on our measurement of the laser diode array which shows a maximum output power of 130 Watt, we expect several Watt output power at 2.8 micron if the laser diode array would be operated at its maximum output power. Comparison between the 2-D results and the 1-D results shows a lower output power and efficiency for the 2-D array. The main reason for the lower efficiency of the 2-D array is probably the wider pump spectrum of the 2-D pump array. The effect of micro-laser efficiency as a function of pump spectrum was investigated by varying the pump wavelength of the laser diode in the 1-D micro-laser array by changing the temperature of the laser diode heatsink from 12.5 to 25 degrees C, as was shown in Figure 19. At 976 nm peak wavelength from the laser diode array, the micro-laser output power is reduced by 40 % as compared to the output power from the micro-laser array pumped at 973 nm. A similar reduction in efficiency is found at wavelengths shorter than 973 nm. These experiments confirm that the lower efficiency of the 2-D micro-laser array with a pump spectrum extending from 969 to 977 nm FWHM is to a large extent related to the relatively wide pump spectrum of the 2-D array. Measurements of the pump spectrum as a function of the position in the near field of the 2-D laser diode arrays shows that the broad spectrum of the 2-D array is related to a broader spectrum of each of the individual lasers and not related to a variation in wavelength over the 2-D pump array elements.

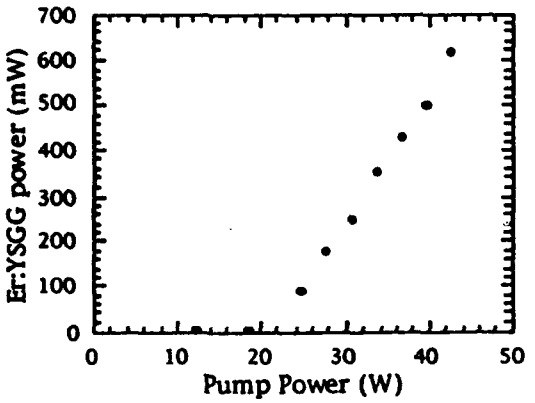

Figure 31: Measured output power at 2.9 μm from the 4 x 12 element Er:YSGG micro-laser array as a function of input pump power at 970 nm. Operating conditions are 4 ms pulse, 5 Hz.

VI. DELIVERABLE

The deliverable under this contract is a 2-D Er:YSGG micro-laser array with the following characteristics:

- Monolithic 2-D surface emitting laser diode array. The output characteristics of this laser diode array are shown in Figures 28 and 29. A maximum output power of 132 W q-cw is demonstrated from the 48 element array, corresponding to an output power of 2.75 Watt per element. The 2-D laser diode array is mounted on a compact water cooled heat sink which requires an external circulating cooler with a pressure of 20 psi and 1 liter/min flow. The laser diode requires a standard laser diode power supply such as the SDL model no 928 or SDL model no 930. For long laser diode lifetime it is recommended to operate the laser below a few percent duty cycle. Although, the laser array has been designed for cw operation and cw operation was demonstrated from individual surface emitters, we have not tested the current laser under cw operations, because of possible lifetime issues.

- Er:YSGG microchip laser with dimensions matched to that of the laser diode array described above. The micro-laser is mounted on a water cooled heat sink. The water cooling of the microchip can be done in series with the cooling of the laser diode.

- The combination of the laser diode array butt coupled to the Er:YSGG micro-laser has demonstrated 0.6 Watt output power at 2.8 micron wavelength, as shown in Figure 31. This output power was achieved under the following operating condition of the laser diode: 100 Amps pump current, 42 watt peak pump power, 4 msec pulse length, 5 Hz repetition rate, and 15° water temperature.

- The deliverable is a prototype laser which requires additional standard mechanical positioners to align the laser diode array to the micro-laser array. After aligning the angles of the micro-laser and the laser diode array such that they are parallel, the distance between the laser diode array and the micro-laser is reduced to approximately 50 micron.

More specifically, the deliverable includes the following parts:

1) Laser diode array mounted on an impingement water cooler, labeled 2D 12*4 SEL s/n 001 The laser diode is approximately 1 by 0.5 cm. Two lasers arrays are mounted on the same 1 by 2 cm^2 heat sink. Only the left array is operational.

2) A copper plate for providing the electric ground contact to the heat sink.

3) A water manifold to allow the connection of standard water tubing to the impingement cooler.

4) An Er:YSGG micro-laser as described in this report, mounted on a copper submount

5) A water cooled copper heatsink for cooling of the Er:YSGG micro-laser.

To install the system:

1) Connect the copper ground contact (2) to the laser diode array (1).

2) Connect the water manifold (3) to the laser diode array (1).

3) Connect the power supply to the laser diode array. The negative contact goes to the top of the diode, the positive contact is connected to the ground plate.

4) Mount the Er:YSGG micro-laser (4) to the water cooled heatsink (5).

5) Connect all cooling to the micro-laser and laser diode (20 psi / 1 l/min)

6) Align the laser diode to the micro-laser with a distance of about 50 micron between the laser diode array surface and the micro-laser array input surface.

VII. CONCLUSIONS

In this work, SDL investigated the operation of 1-D and 2-D micro-laser arrays. The micro-laser experiments cover single micro-lasers and linear and 2-D micro-laser arrays with output wavelengths around 1 and 3 microns. The experiments demonstrate the suitability of monolithic 2-D laser diode pump arrays as a pump source for 2-D micro-laser arrays. The monolithic, surface emitting, 2-D laser diode arrays developed under this program with over 130 Watt q-cw output power, are the highest power monolithic laser diode arrays demonstrated to date. Our research suggests that high power 2-D micro-laser arrays may be developed for applications which require a high power and high brightness laser source for applications such as material processing and medical.

Two different solid state materials were investigated, (i) Yb:YAG pumped at 940 nm and lasing at 1.03 micron and Er:YSGG pumped at 940 nm and lasing at 2.8 micron. However our experimental results can easily be extended to a large number of other micro laser with different pump and lasing wavelengths. The Yb:YAG experiments include the demonstration of single micro-lasers with up to 200 mW q-cw output power. The output power and efficiency of these Yb:YAG lasers is lower than theoretically predicted. Comparison with other research labs show experimental results that vary widely using similar experimental set-ups for Yb:YAG. Possibly, there is a materials issue associated with the relatively new Yb:YAG system. If Yb:YAG can be made to operate consistently it is a attractive alternative for Nd:YAG.

The experiments with Er:YSGG included both experiments with conventional, linear surface emitting laser arrays as well as novel surface emitting laser diode arrays. The linear array experiments also demonstrated that micro-optics between the laser diode array and the micro-laser array may improve the output power and efficiency from the micro-laser array. Over 900 mW cw output power was demonstrated from a 12 element linear Er:YSGG micro-laser array based on a 15 Watt laser bar with coupling optics between the laser diode array and the micro-laser array. The 2-D Er:YSGG micro-laser array are based a 48 element surface emitting laser array. Over 600 mW q-cw output power has been demonstrated at 42 Watts pump power, limited by the power supply. The efficiency and output power may be increased by a factor of 4 with used of proper coupling optics between the laser diode array and the micro-laser and the use of a laser diode array with a 1-2 nm spectrum as opposed to the 7 nm spectrum from the current laser diode array. In addition the laser diode can be operated up to 130 Watt with a suitable power supply. Based on these improvements we expect 3-5 Watt output power from these 2-D laser diode arrays. Further scaling in output power is possible by increasing the overall area of the laser diode array.

VIII. ACKNOWLEDGMENTS

This work was carried out under ARPA contract #MDA-972-92-C-047. The principle investigators in this program were Dr. Robert G. Waarts, Dr. Derek Nam and Dr. Steve Sanders. In addition, Dr. David Welch and Dr. David Mundinger acted as technical consultants. Dr. James Harrison at SEO was involved with some of the calculations and the linear Er:YSGG micro-laser experiments. The Er:YSGG micro-laser for the 2-D micro-laser array experiments at SDL was made available to this program by SEO.

IX. REFERENCES

1. J.J. Zayhowski and A. Mooradian, "Single-frequency microchip Nd lasers," Optics Letters, vol. 14, pp. 24-26, 1989.

2. J. A. Keszenheimer, S. F. Root and K. F. Wall, "Q-switched, one dimensional Nd:YAG microchip laser array," CLEO 93 postdeadline paper CPD11.

3. J. Harrison and R.J. Martinsen, "Operation of linear micro-laser arrays near 1 micron, 2 micron and 3 micron", Proceeding Advanced Solid State Laser Conference, Salt Lake City, February 1994.

4. C. D. Nabors, A. Sanchez and A. Mooradian, "High power, continuous-wave, Nd:YAG microchip laser array," Optics Letters, vol. 17, pp. 1587-1589, 1992.

5. W. D. Goodhue, J. P. Donnelly, C. A Wang, G. A. Lincoln, K. Rauschenbach, R. J. Bailey, and G. D. Johnson, "Monolithic two dimensional surface-emitting strained-layer InGaAs/AlGaAs and AlInGaAs/AlGaAs diode laser arrays with over 50 % differential quantum efficiencies," *Appl. Phys. Lett.*, 59, (6), pp 632-634 (1991).

6. S.S. Ou, M. Jansen, J.J. Yang, L.J. Mawst, and T.J. Roth, "High power operation of InGaAs/GaAs surface emitting laser with 45 degree intracavity micro-mirrors," *Appl. Phys. Lett.*, 59, (17), pp. 2085-2087 (1991).

7. M. Jansen, J.J. Yang, S.S. Ou, M. Sergant, L. Mawst, J. Rozenbergs, J. Wilcox, and D. Botez, "Monolithic two-dimensional surface emitting laser arrays mounted in the junction down configuration," *Appl. Phys. Lett.*, 59, (21), pp. 2663-2665 (1991).

8. J. P. Donnelly, W. D. Goodhue, C. A. Wang, R. J. Bailey, G. A. Lincoln, G. D. Johnson, L. J. Missaggia, and J. N. Walpole, *IEEE Photonics Technol. Lett.*, 5, (7), pp. 747-750 (1993).

9. J. P. Donnelly, W. D. Goodhue, C. A. Wang, R. J. Bailey, G. A. Lincoln, G. D. Johnson, L. J. Missaggia, and J. N. Walpole, "CW operation of monolithic arrays of surface emitting AlGaAs diode lasers with dry-etched vertical facets and parabolic deflecting mirrors," *IEEE Photonics Technol. Lett.*, 5, (10), pp. 1146-1149 (1993).

10. D. W. Nam, R. G. Waarts, D. F. Welch, J. S. Major, Jr., and D. R. Scifres, "Operating characteristics of high continuous power (50W) two-dimensional surface-emitting laser array," *IEEE Photonics Technol. Lett.*, **5**, (7), pp. 281-284 (1993).

11. J. Harrison and R. J. Martinsen, "Thermal modeling for mode-size estimation in micro-lasers with application to linear arrays in Nd:YAG andTm,Ho:YLF,"IEEE J. Quantum Electronics, to be published.

X. RELATED PUBLICATIONS

1) D. Nam, S. Sanders, R. G. Waarts and D. F. Welch, "130 Watt monolithic surface emitting laser arrays, :submitted toe IEEE Photonics Technologies Letters

2) R. Waarts, D. Nam, S. Sanders, J. Harrison and B. J. Dinerman, "2-D Er:YSGG micro-laser array pumped with monolithic 2-D laser diode array, " manuscript in preparation.